

# Ventral attention network connectivity is linked to cortical maturation and cognitive ability in childhood

Received: 19 May 2023

Accepted: 18 July 2024

Published online: 23 August 2024

 Check for updates

Hao-Ming Dong<sup>1</sup>✉, Xi-Han Zhang<sup>1</sup>, Loïc Labache<sup>1</sup>, Shaoshi Zhang<sup>2</sup>, Leon Qi Rong Ooi<sup>2</sup>, B. T. Thomas Yeo<sup>2,3,4</sup>, Daniel S. Margulies<sup>5</sup>, Avram J. Holmes<sup>6,10</sup>✉ & Xi-Nian Zuo<sup>7,8,9,10</sup>✉

The human brain experiences functional changes through childhood and adolescence, shifting from an organizational framework anchored within sensorimotor and visual regions into one that is balanced through interactions with later-maturing aspects of association cortex. Here, we link this profile of functional reorganization to the development of ventral attention network connectivity across independent datasets. We demonstrate that maturational changes in cortical organization link preferentially to within-network connectivity and heightened degree centrality in the ventral attention network, whereas connectivity within network-linked vertices predicts cognitive ability. This connectivity is associated closely with maturational refinement of cortical organization. Children with low ventral attention network connectivity exhibit adolescent-like topographical profiles, suggesting that attentional systems may be relevant in understanding how brain functions are refined across development. These data suggest a role for attention networks in supporting age-dependent shifts in cortical organization and cognition across childhood and adolescence.

The human brain undergoes a series of staged developmental cascades across childhood and adolescence, progressing from unimodal somatosensory/motor and visual regions through the transmodal association cortex territories that support complex cognitive functions<sup>1–3</sup>. Evidence for the scheduled timing of these neurodevelopmental events has emerged across biological scales, from regional profiles of cellular maturation<sup>4</sup>, synapse formation and dendritic pruning<sup>5</sup>, and intracortical myelination<sup>6</sup> through macroscale morphological features including folding patterns<sup>7</sup> and associated areal expansion<sup>8</sup>. These processes are

imbedded within age-dependent anatomical changes across lifespan<sup>9</sup>, particularly the prolonged development of association cortex territories. In parallel, substantial progress has been made characterizing the organization<sup>10,11</sup> and spatiotemporal maturation of large-scale functional systems across the cortex<sup>12,13</sup>. Here, *in vivo* imaging work strongly supports the development of a hierarchical axis, or gradient, of cortical organization, with association territories anchored at the opposite end of a broad functional spectrum from primary sensory and motor regions<sup>14</sup>. Despite clear evidence for age-dependent shifts

<sup>1</sup>Department of Psychology, Yale University, New Haven, CT, USA. <sup>2</sup>Centre for Sleep and Cognition and Centre for Translational Magnetic Resonance Research, Yong Loo Lin School of Medicine, Singapore, National University of Singapore, Singapore, Singapore. <sup>3</sup>Department of Electrical and Computer Engineering, National University of Singapore, Singapore, Singapore. <sup>4</sup>N.1 Institute for Health and Institute for Digital Medicine, National University of Singapore, Singapore, Singapore. <sup>5</sup>Centre National de la Recherche Scientifique, Frontlab, Institut du Cerveau et de la Moelle Epinière, Paris, France.

<sup>6</sup>Department of Psychiatry, Brain Health Institute, Rutgers University, Piscataway, NJ, USA. <sup>7</sup>State Key Laboratory of Cognitive Neuroscience and Learning, Beijing Normal University, Beijing, China. <sup>8</sup>National Basic Science Data Center, Beijing, China. <sup>9</sup>Developmental Population Neuroscience Research Center, IDG/McGovern Institute for Brain Research, Beijing Normal University, Beijing, China. <sup>10</sup>These authors contributed equally: Avram J. Holmes, Xi-Nian Zuo.

✉e-mail: [donghaomingnd@gmail.com](mailto:donghaomingnd@gmail.com); [avram.holmes@rutgers.edu](mailto:avram.holmes@rutgers.edu); [xinian.zuo@bnu.edu.cn](mailto:xinian.zuo@bnu.edu.cn)

in the macroscale organization of the cortex from childhood through adolescence, the manner and extent to which specific functional networks may contribute to the widespread process of cortical maturation remains to be determined.

The focused study of discrete functional circuits has provided foundational insights into core maturational processes. For example, discoveries have linked hierarchical changes within amygdala- and ventral striatal-medial prefrontal cortex (mPFC) circuitry to the development of emotional and social functioning in adolescence<sup>1,3,15,16</sup>. Yet, the maturational refinement of these subcortical-cortical circuits does not occur in isolation. Rather, they are embedded within a broad restructuring of functional systems across the cortical sheet<sup>17</sup>. Here, areal and network boundaries become more clearly defined throughout development<sup>18</sup>, while the predominance of local connectivity patterns in childhood gradually gives way to long distance, integrative, connections in adolescence<sup>13,19,20</sup>. This reflects a developmental transition from an anatomically constrained organizational motif to a topographically distributed system<sup>21</sup>. In children, this complex functional architecture is situated within the unimodal cortex, between somatosensory/motor and visual regions. Conversely, adolescents transition into an adult-like gradient, anchored at one end by unimodal regions supporting primary sensory/motor functions and at the other end by the association cortex<sup>14</sup>. Whereas the organizational profiles of large-scale cortical networks are distinct across childhood and adolescence<sup>22</sup>, the extent to which developmental changes within select functional couplings may contribute to the drastic reorganization in the brain hierarchy is an open question. By one view, the developmental transition from unimodal through association cortices reflects the coordinated and shared influence of maturational changes across several functional systems spanning the entire connectome. An alternative, although not mutually exclusive, possibility is that specific brain networks may play a preferential role in the widespread developmental refinement of cortical connectivity.

Individual cortical parcels are organized functionally along a global gradient that transitions from somato/motor and visual regions at one end to multimodal association cortex at the other<sup>23</sup>. The hierarchical nature of these functional relationships reflects a core feature of brain organization in both adolescents<sup>14</sup> and adults<sup>23</sup>. Incoming sensory information undergoes a process of extensive elaboration and attentional modulation as it cascades into deeper layers of cortical processing. Visual system connectivity, as one example, moves along the dorsal and ventral visual streams, uniting within aspects of the dorsal and ventral attention networks including the anterior insula, superior parietal cortex, and operculum parietal before eventually filtering through multimodal convergence zones, particularly within the default network<sup>24</sup>. Although speculative, these data suggest a possible preferential role for sensory orienting and attentional systems in the integrity of the information processing hierarchies in the human brain. Intriguingly, there is mounting evidence to suggest the staged development of a ventral attention network, encompassing aspects of anterior insula, anterior prefrontal cortex and anterior cingulate cortex<sup>11,25</sup> (see also cingulo-opercular network<sup>26</sup> and salience network<sup>27</sup>) that follows the age-dependent shifts in cortical organization across childhood and adolescence<sup>14</sup>. The salience/ventral attentional network, together with frontoparietal network, have been proposed to constitute a dual-network system for the 'top-down' and 'bottom-up' processing necessary for adaptive behavioral responses<sup>26,28,29</sup>, supporting the functional propagation of information across primary somato/motor, visual and auditory cortex through the default network<sup>24</sup>. These dissociable attentional and control systems are interconnected in children but later segregate over the course of adolescence to eventually form the parallel architectures that support adaptive behavior in adulthood<sup>18</sup>. These data suggest that the attention system may play a preferential role in the transformative brain changes occurring throughout childhood and adolescence. Recent work has also revealed that the lateralization of functional gradients may coincide with attention

system lateralization<sup>30</sup>. As such, characterizing the relationships linking attention network connectivity and age-dependent changes in macroscale brain organization would provide a tremendous opportunity to understand how the functional architecture of cortex is shaped and sculpted across the human lifespan. In turn, this would provide the opportunity to examine how the hierarchical reorganization of the cortical sheet may contribute to the emergence of cognitive and emotional abilities that mark the transition from childhood to adolescence.

In the present study, we examined the extent to which specific functional networks may serve to underpin the age-dependent maturation of functional gradient patterns across the cortical sheet. To address this open question directly, we first established the cortical territories exhibiting pronounced functional changes in a longitudinal sample of children and adolescents, revealing the preferential presence of developmental shifts within the ventral attention network. Follow-up analyses excluding regions exhibiting the maximal developmental change in children resulted in the emergence of adolescent-like gradient patterns, suggesting that ventral attention territories may play a core role in the expression of adolescent-like connectivity gradients. Moreover, across independent datasets, children with low ventral attention connectivity exhibited a profile of cortical organization that closely resembles previous reports in adolescents and adults. Highlighting the importance of attention network connectivity in cognitive functioning, standardized measures of intelligence linked with reduced attention network degree centrality in children and adolescents. Collectively, these data suggest that ventral attention system functioning in childhood and adolescence may underpin the developmental reorganization and maturation of functional networks across the cortical sheet.

## Results

### Ventral attention network territories demonstrate high degree centrality and pronounced shifts across development

Vertex-level functional connectivity (FC) matrices ( $20,484 \times 20,484$ ) were first generated using the data provided by the Chinese Color Nest Project (CCNP)<sup>21,31</sup>. In line with previous work<sup>10,11,14</sup>, the top 10% connections of each vertex were retained to enforce sparsity. Degree centrality maps for both children (6–12 years of age;  $n = 202$ ) and adolescents (12–18 years of age;  $n = 176$ ) were generated to characterize the broad organizational properties of the functional connectome across development (Fig. 1a,b). Here, degree centrality reflects the count of above-threshold connections for a given vertex compared with all other vertices (Methods).

The observed profiles of degree centrality were highly similar between children and adolescents (Pearson's  $r = 0.947$ ,  $P_{\text{spin}} \leq 0.001$ ). Significance was established using permuted spin tests, which preserve the spatial autocorrelation structure of the data<sup>32</sup>. Heightened degree centrality values in both children and adolescents were preferentially evident in aspects of the ventral attention network, including portions of anterior insula, mPFC and anterior cingulate cortex/midline supplementary motor area (Fig. 1). Increased degree centrality was also present in adolescents within default network territories, including portions of posterior inferior parietal lobule, posterior cingulate cortex and precuneus. Additionally, visual system areas, including superior and transverse occipital sulcus at the boundary between dorsal and visual network, demonstrated high degree centrality values. Conversely, primary somatosensory and motor areas as well as regions within the lateral prefrontal cortex and temporal lobe exhibited relatively low degree centrality. Broadly, these data reflect the presence of dense connectivity within medial and posterior territories along the cortical sheet, while relatively low centrality was evident in lateral prefrontal and somato/motor areas, highlighting a stable pattern of degree centrality across childhood and adolescence.

Degree centrality broadly summarizes profiles of cortical connectivity, to examine developmental changes in FC strength at the vertex level, we calculated the associated Euclidean distance in FC similarity between

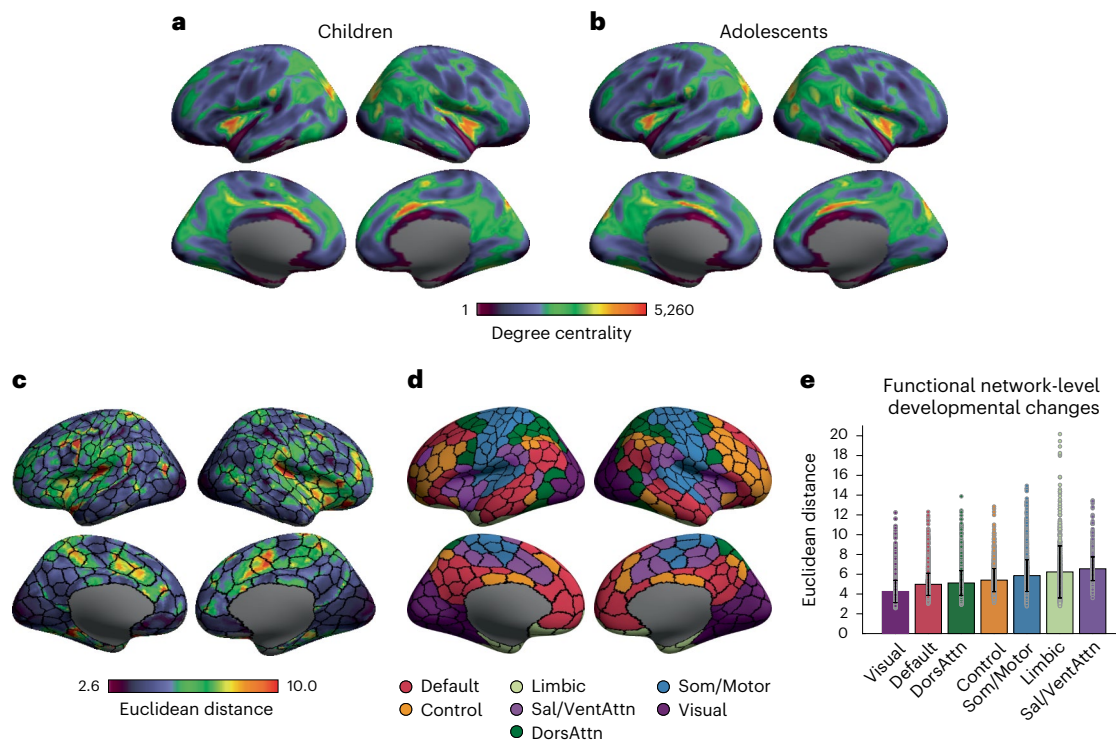


**Fig. 1 | Ventral attention network areas demonstrate high population-level degree centrality but pronounced functional changes across development.** **a, b**, Degree centrality maps in children (**a**) and adolescents (**b**) reveal consistent dense connectivity in ventral attention network areas throughout development. Scale bar reflects the count of above-threshold connections from a given vertex compared with all other vertices. Larger values indicate higher degree centrality. **c**, Euclidean distance of the functional connectome at each vertex between children and adolescents reveals a clear switch within the ventral attention network. Larger values indicate greater dissimilarity. **d**, Regions based

on the Schaefer et al., 400-parcel<sup>33</sup> atlas and colored by the Yeo et al., seven-network solution<sup>11</sup>. **e**, Bar graph reflects changes in the Euclidean distance of functional connectome at network level (mean network values ± s.e.m.). The ventral attention network ( $6.5518 \pm 1.2002$ ) shows the largest developmental change whereas the visual ( $4.2584 \pm 1.1257$ ) and default ( $4.9813 \pm 1.1207$ ) networks are most stable between children and adolescents. DorsAttn, dorsal attention ( $5.1157 \pm 1.2499$ ); Sal, salience; Som/Mot, somato/motor ( $5.8618 \pm 1.6067$ ); VentAttn, ventral attention; Control ( $5.4065 \pm 1.1681$ ); and Limbic ( $6.2337 \pm 2.6297$ ).

children and adolescents (Fig. 1c). Despite the presence of broadly consistent population-level patterns of degree centrality, analyses revealed spatially nonuniform shifts in hub regions of FC across groups. The maximum developmental changes were anchored within the ventral attention network (Fig. 1c–e), encompassing aspects of anterior and posterior insula as well as cingulate cortex<sup>11,33</sup>. One-way analysis of variance revealed the presence of between-network differences ( $F = 790.94$ ,  $d.f. = 6$ ,  $P \leq 0.001$ ), with increased Euclidean distance in the ventral attention network relative to other networks (see multiple comparisons results in Supplemental Table 2). Previous work indicates that maturational age broadly follows the theorized hierarchy of cortical information processing<sup>23</sup>, with somato/motor and visual networks maturing in childhood, while medial prefrontal aspects of default and limbic networks peak later during adolescence<sup>14,34</sup>. However, in the present analyses, the default network exhibited relatively less developmental change in Euclidean distance between groups, followed by visual network (Fig. 1e). Although speculative, these data suggest the presence of specific network-level similarities in connectivity between children and adolescents that may precede broader age-dependent shifts in the macroscale organization of cortex, highlighting the need to consider the manner in which individual functional networks (for example, default and attention) are embedded within the broader functional architecture of the brain.

#### A core role for the ventral attention network in the macroscale organization of cortex across childhood and adolescence

The transition from childhood to adolescence is marked by pronounced changes in the functional organization of cortex<sup>14,22</sup>. Broadly, this is reflected in the presence of age-dependent transitions across

macroscale gradients that extend from unimodal (somato/motor and visual) regions through the cortical association areas that support complex cognition<sup>2,3,15,16</sup> (Fig. 2a). Of note, such a transition is observed not only when restricting analyses to retain the top 10% connections of each vertex to enforce sparsity, but also revealed by when varying sets connections are included in the gradient analyses. Here, the primary transmodal gradient emerges in a higher percentile of excluded connections at each vertex (90%) in adolescents than in children (85%; Extended Data Fig. 1). Next, we examined whether age-dependent alterations in ventral attention network connectivity might partly account for the maturation of the cortical processing hierarchy as reflected in these overlapping organizing axes, or gradients. Brain areas with maximum differences in Euclidean distance were extracted (Fig. 2b; Methods), and then removed from brain connectivity matrix while we rederived the functional gradients. Here, diffusion map embedding<sup>10,35,36</sup> was used to decompose participant-level connectivity matrices into a lower dimensional space. The resulting functional components, or gradients, reflect dissociable spatial patterns of cortical connectivity ordered by the variance explained in the initial FC matrix<sup>10,14</sup>.

As identified in our previous study<sup>14</sup>, the primary gradient in children closely matches the second gradient in adolescents and adults. Here, dropping ventral attention areas (a simulation of lesion) generates adolescent- and adult-like gradient architectures in children. The simulated removal of ventral attention network regions led to the formation of a primary gradient in children that closely assembles the first gradient in both adolescents ( $r = 0.68$ ,  $P_{\text{spin}} \leq 0.001$ ) and adults ( $r = 0.84$ ,  $P_{\text{spin}} \leq 0.001$ ). The rederived second gradient in children most closely assembled the second gradient in both adolescents ( $r = 0.66$ ,



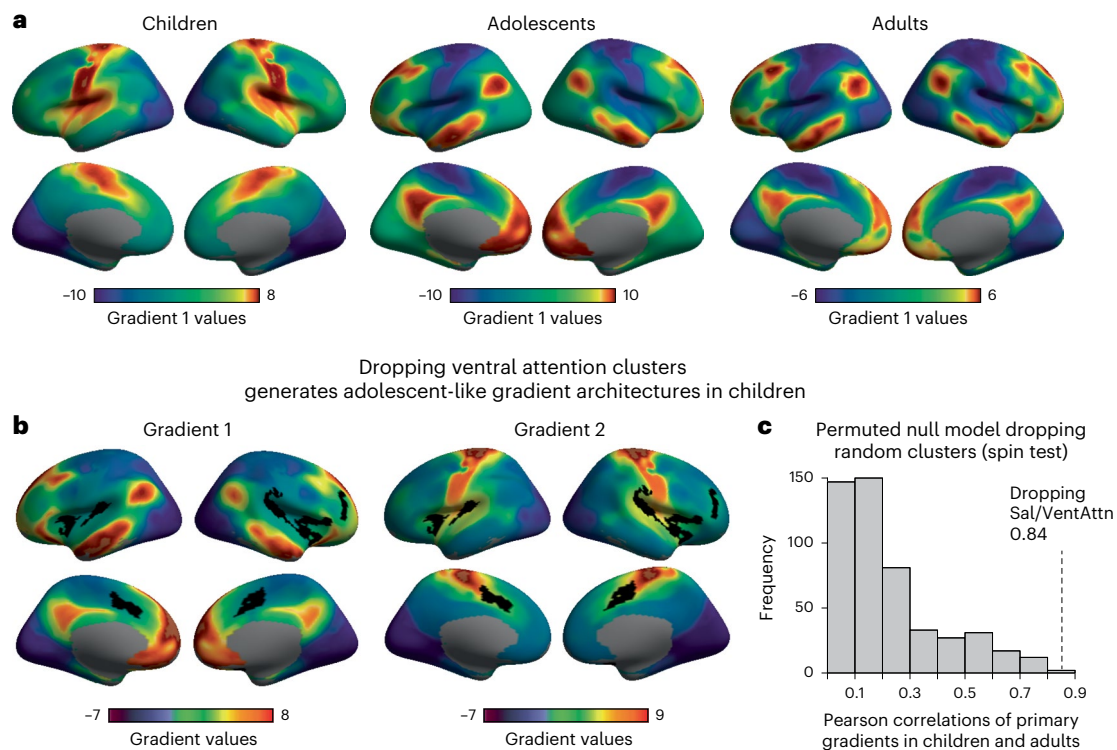


**Fig. 2 | Ventral attention territories play a core role in the expression of adolescent-like connectivity gradients.** **a**, The principal cortical gradients of connectivity in children, adolescents (data from ref. 14) and adults (data from ref. 10). **b**, Clusters with maximum developmental changes in Euclidean distance were extracted (Fig. 1c), denoted as black on the cortical surface. Associated vertices were then dropped from the cortical connectome in the child group before rederiving the gradients. Results reveal that default and visual networks anchor the extremes along the principal gradient (Gradient 1), mirroring the principal gradient in both adolescents ( $r = 0.68$ ,  $P_{\text{spin}} \leq 0.001$ , two-sided spin test) and adults ( $r = 0.84$ ,  $P_{\text{spin}} \leq 0.001$ , two-sided spin test). In children, the rederived second gradient (Gradient 2) revealed a unimodal architecture separating somato/motor network from visual network, which closely corresponds to

the second gradient in both adolescents ( $r = 0.66$ ,  $P_{\text{spin}} \leq 0.001$ , two-sided spin test) and adults ( $r = 0.85$ ,  $P_{\text{spin}} \leq 0.001$ , two-sided spin test). Here, the color scale represents the gradient values across the cortical surface. Vertices with similar colors indicate similarities in their functional connectome. **c**, To further assess the significance of the results, we constructed a permutated null model in the present data. Clusters with same size and shape as in **b** but shuffled locations on the cortical sheet were generated and excluded from analyses in the child group 500 times. For each shuffle, the principal gradient was extracted and compared with the principal gradient in adults. The permutated null model shows only one case revealing a higher correlation than that observed in the real data, the x axis indicates the absolute correlation values, the y axis indicates the frequency of correlations, and the dotted line refers to the hypothesis being tested.

$P_{\text{spin}} \leq 0.001$ ) and adults ( $r = 0.85$ ,  $P_{\text{spin}} \leq 0.001$ ). However, while the primary gradient derived from ventral attention network simulated lesioned data in children broadly recapitulated the primary gradient in adults<sup>10</sup>, several inconsistencies were observed. Notably, in the simulated lesioned data from the child group, one end of the primary gradient of connectivity was anchored in the visual areas, with the regions at the other end encompassed broad swaths of the association cortex. Previous work in adults has revealed visual territories along with somato/motor and auditory cortex serve to anchor one end of the primary cortical gradient<sup>10</sup>. Additionally, although the second gradient derived from ventral attention network simulated lesioned data in children closely resembles the second gradient in adults, a muted default network profile can still be observed. While the dropped clusters are not anchored at the extreme end of the primary gradient in children (Fig. 2a), it is densely connected and spatially adjacent to somato/motor territories. Further control analysis revealed that areas within ventral attention network contributed primarily to the reversal in gradients. Although speculative, dropping of ventral attention vertices from the gradient analyses may decrease the number of functional connections attributed to somato/motor network, indirectly shifting its position along the gradient spectrum.

Most vertexes from the dropped clusters were from the ventral attention (45.96%) and somato/motor (36.57%) networks. Accordingly, the observed transition to an adolescent- and adult-like functional architecture in children may reflect an artifact resulting from lesioning

the data in a manner that removes aspects of the unimodal territories that anchor the primary gradient in children (Fig. 2a). To address this possibility and identify the primary drivers of adolescent-like profiles of brain function in children, we subdivided the dropped clusters into two categories: clusters falling within the borders of the somato/motor network and clusters outside the somato/motor network. Gradients were then rederived in the child group to explore the consequences associated with the individual removal of each cluster component. The removal of somato/motor cluster preserves the developmentally typical gradient architecture in children; the first gradient closely resembles the second gradient in adolescents ( $r = 0.94$ ,  $P_{\text{spin}} \leq 0.001$ ) and adults ( $r = 0.91$ ,  $P_{\text{spin}} \leq 0.001$ ), whereas the second gradient closely resembles the first gradient in adolescents ( $r = 0.95$ ,  $P_{\text{spin}} \leq 0.001$ ) and adults ( $r = 0.91$ ,  $P_{\text{spin}} \leq 0.001$ ). Conversely, and consistent with the analyses reported above (Fig. 2b), dropping the cluster outside somato/motor network led to the generation of an adolescent- and adult-like gradient architecture in children. Here, the first gradient in children matched the first gradient in adolescents ( $r = 0.78$ ,  $P_{\text{spin}} \leq 0.001$ ), whereas the second gradient in children resembled the second gradient in adolescents ( $r = 0.78$ ,  $P_{\text{spin}} \leq 0.001$ ), that is, dropping the clusters outside somato/motor network in children results in a gradient organization that resembles previous reports in adolescents.

We next examined the extent to which the observed elimination of age-dependent shifts in the macroscale organization of the cortex is specific to the removal of ventral attention network-dominated vertices.

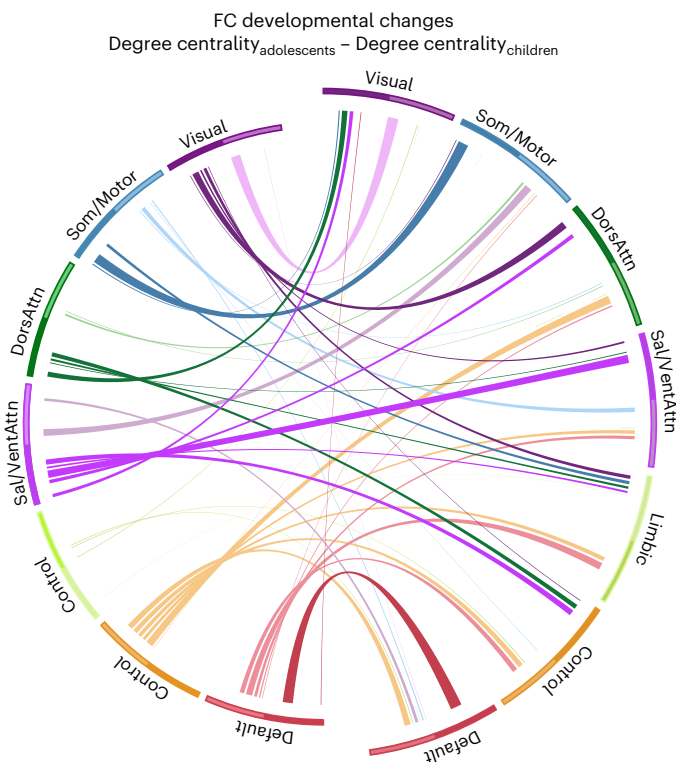


**Fig. 3 | Developmental shifts in FC between childhood and adolescence.** Differences in network-level connectome (the degree centrality matrix of adolescents minus the degree centrality matrix of children) functioning between children and adolescents are demonstrated in a chord diagram. For each network, the number connections within the top 10% of each vertex are first summarized at network level, displayed as the links from right half circle with larger radius to left half circle with smaller radius. Reflecting the asymmetrical nature of the thresholded connectivity matrix, links from the left to right half circle indicate the connections within each network that are included in the top 10% of connections to other vertices. Line width highlights the number of connections, with broader lines indicating increased connectivity. Dark colored lines indicate increased values in adolescents relative to children. Light color lines indicate decreased values in the adolescent group.

Here, we generated 500 null models in the child group with clusters dropped at random locations across the cortical sheet, but with shapes and sizes that match the ventral attention network vertices (reflecting the maximum differences in Euclidean distance between children and adolescents). For each random model, the first and second gradients of the child group were extracted and correlated with the corresponding first and second gradients in adults. Providing evidence for the role of the ventral attention network in the formation of adult-like gradient architectures in children, for the primary gradient the observed correlation was greater than the correlations from the null distribution ( $P \leq 0.002$ ) across 499 of 500 permutations (Fig. 2c). For the second gradient, the observed correlation was greater than the correlations from the null distribution ( $P \leq 0.001$ ) across all 500 permutations. While the present analyses are consistent with a core role for the ventral attention network in age-dependent changes in the macroscale organization of the cortex, longitudinal future work should examine the role of person level factors and possible relationships linking large-scale gradient transitions with shifts in attention network functioning across development.

### Cortical development is linked to a pattern of heightened within-ventral-attention-network connectivity

Extending upon the previous Euclidean distance analyses, connectome-level changes in FC between children and adolescents

are displayed in a chord diagram (Fig. 3) and grouped into networks according to Yeo's seven-network solution<sup>11</sup>. These data reveal broad increases in within-network connectivity for the ventral attention, somato/motor and default networks as well as a general flattening of cross-network connectivity across development. The within-network connections for the ventral attention, between-network connections for the dorsal attention and visual networks were increased, while other between-network connectivity with somato/motor, limbic, frontoparietal and default networks are decreased from childhood to adolescence. Individual developmental changes were examined by a linear mixed effect (LME) model. Decreased between-network connectivity for the somato/motor network was observed ( $P \leq 0.05$ ), whereas heightened between-network connectivity was evident for the visual ( $P \leq 0.05$ ), dorsal attention ( $P \leq 0.001$ ), limbic ( $P \leq 0.05$ ) and frontoparietal control ( $P \leq 0.01$ ) networks. The degree centrality of ventral attention network increased with age in children ( $P \leq 0.05$ ), stabilizing in adolescence where no other age-related associations were revealed in within-network connections for ventral attention network.

When considering other large-scale association networks, the present analyses suggest a pattern where default network connectivity with other functional systems is pruned during development, indicating a bias towards within-network connectivity and an associated differentiation from other network processes. A developmental profile that may coincide with the emergence of the default network at the apex of the network hierarchy in adolescence. Conversely, the frontoparietal control network exhibited increased connectivity with dorsal and ventral attention networks in adolescents, suggesting a potential association between cognitive processes and attentional resources allocation during development.

### Attention network connectivity links with cognitive ability and reveals the presence of adult-like gradient architectures in childhood

The analyses above provide evidence for a relationship between ventral attention network connectivity and the formation of adult-like gradient architectures in children. Substantial connectome-level changes were also observed in heightened within-network FC and degree centrality of ventral attention network (Fig. 3). However, it is not yet clear the extent to which individual variability in attention network functioning may link with the adult-like gradient architectures across development. To distinguish it from the typical developmental pattern, we refer to these early-emerging adult-like gradient architectures as an 'accelerated maturation pattern.' To examine this potential relationship, we divided participants into subgroups based on their individual ventral attention network connection counts (Fig. 4a). Here, to avoid potential bias introduced by confounding factors such as scan parameters, population and preprocessing steps, the group split was determined based on the median connection count in the CCNP oldest participants (>17 years of age; dotted line in Fig. 4a) rather than independent adult population samples. Participants with fewer connections than this median value were assigned to a low ventral attention group (child  $n = 95$  adolescent  $n = 76$ ), all other participants were assigned to a high ventral attention group (child  $n = 107$ ; adolescent  $n = 100$ ). The gradients were then rederived for high and low attention groups across both children and adolescents. No significant associations were observed between the degree centrality of ventral attention network and demographic factors including in age ( $P = 0.45$ ), gender ( $P = 0.82$ ) and head motion ( $P = 0.87$ ). Further comparisons reveal matched demographic features between child the high and low ventral attention groups in age ( $P = 0.0572$ ), gender ( $P = 0.7716$ ) and head motion ( $P = 0.5346$ ).

In adolescents, both the primary ( $r = 0.98$ ,  $P_{\text{spin}} \leq 0.001$ ) and secondary ( $r = 0.99$ ,  $P_{\text{spin}} \leq 0.001$ ) gradient architectures were consistent within the low and high ventral attention network participants (Fig. 4b,c). For children with high salience and ventral attention connectivity, their functional organization follows the typical pattern of

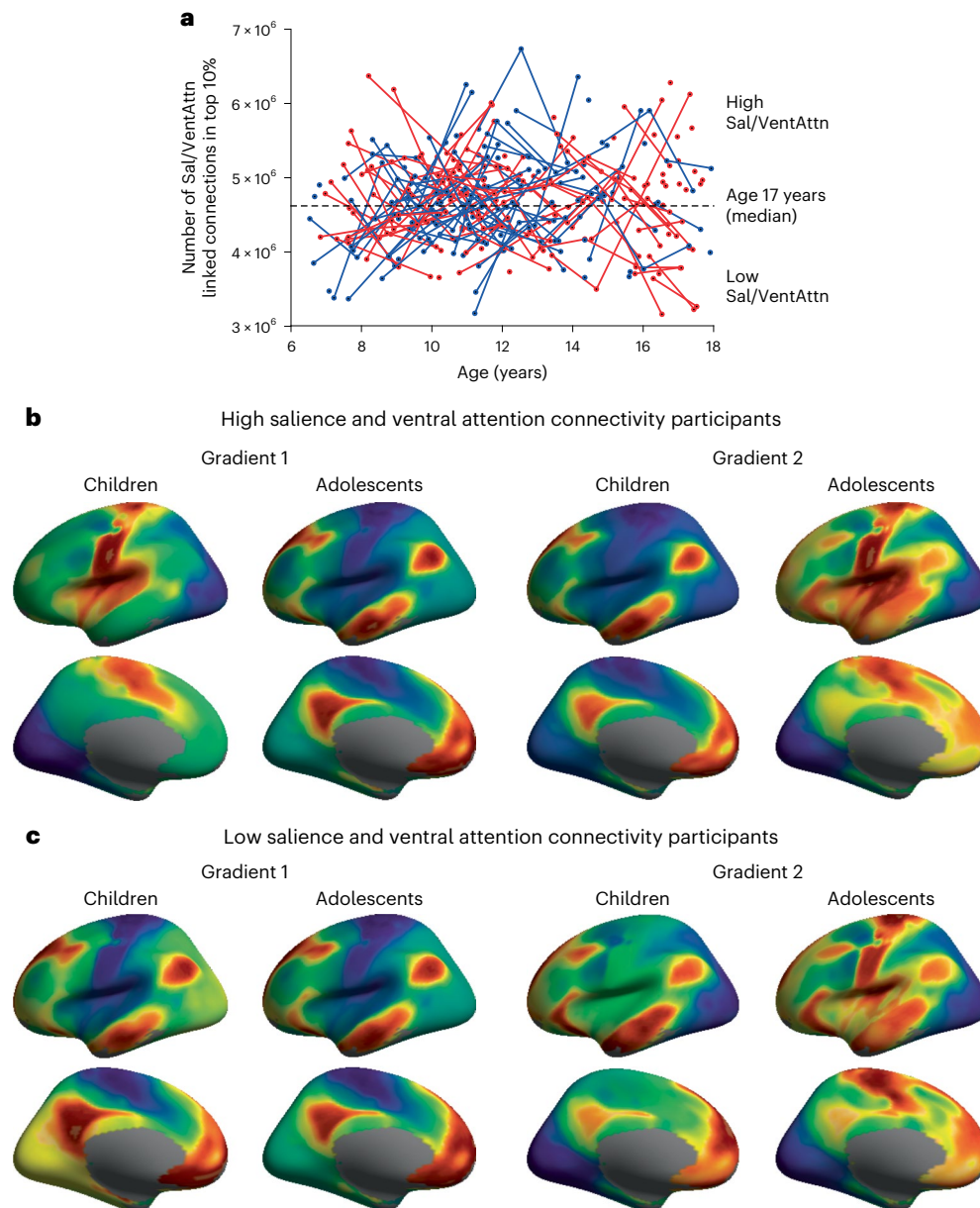


**Fig. 4 | Individual differences in ventral attention network connectivity reveal a functional profile that resembles accelerated cortical maturation in some children.** **a**, The number of functional connections linked with ventral attention network at individual level. Blue, Male participants; red, female participants. Repeated imaging sessions within the same participants are linked by lines. The *x* axis represents age range (6–18 years). The *y* axis reflects the number of connections that are linked to the ventral attention network following thresholding. Participants were divided into high and low ventral attention connectivity groups according to the median value in 17-year-old participants (dotted line). **b**, Gradient maps in high ventral attention connectivity groups reveal typical patterns identified in our previous work in both children and adolescents<sup>14</sup>. **c**, Gradient maps in low ventral attention connectivity groups reveal an accelerated maturation process in children, with both the primary

and secondary gradients demonstrated a transmodal architectures. Functional organization was broadly preserved across the high and low attention groups in adolescents, with a subtle muting of the ventral attention gradient values in the low attention participant group. Here, the color scale represents the gradient values across the cortical surface. Vertices with similar colors indicate similarities in their functional connectome. The primary gradient maps in high and low ventral attention connectivity groups derived from longitudinal data. These surface maps display a developmentally normative pattern of gradient reversals in the high ventral attention group children, later scanned in adolescence. Conversely, low ventral attention group children exhibit a stable adolescent-like gradient architecture in both childhood and adolescence. See Extended Data Figs. 2 and 3 for longitudinal analyses of Gradient 1 and Gradient 2 in both hemispheres.

brain maturation<sup>14</sup> (Fig. 2a). Here, the primary gradient in the high ventral attention children matched the secondary gradient in both adolescents ( $r = 0.89$ ,  $P_{\text{spin}} \leq 0.001$ ) and adults ( $r = 0.91$ ,  $P_{\text{spin}} \leq 0.001$ ), while the second gradient in high ventral attention children matched the primary gradient in both adolescents ( $r = 0.89$ ,  $P_{\text{spin}} \leq 0.001$ ) and adults ( $r = 0.91607$ ,  $P_{\text{spin}} \leq 0.001$ ). In these children, somato/motor areas were anchored at the opposite extreme from visual regions, revealing

a unimodal dominant gradient architecture. However, in children with low ventral attention connectivity, we observed a developmentally accelerated pattern of gradient organization that broadly matches the primary and secondary gradients identified previously in both adolescents (Gradient 1:  $r = 0.93$ ,  $P_{\text{spin}} \leq 0.001$ ; Gradient 2:  $r = 0.92$ ,  $P_{\text{spin}} \leq 0.001$ ) and adults (Gradient 1:  $r = 0.68$ ,  $P_{\text{spin}} \leq 0.001$ ; Gradient 2:  $r = 0.65$ ,  $P_{\text{spin}} \leq 0.001$ ).



Permutation analyses were conducted to examine the significance of the dissociable gradient architectures across the groups. Here, 95 and 107 child participants were assigned randomly to two groups corresponding to the number of participants in low and high ventral attention child group for 500 permutations. In the adolescent group, 76 and 100 participants were assigned randomly to two groups corresponding to the number of participants in low and high ventral attention adolescent group for 500 times; the gradient maps were then recomputed and the associated variances extracted to generate a set of null models.

Children with low ventral attention connectivity exhibit a gradient organization that broadly matches the primary and secondary gradients identified previously in both adolescents and adults. Conversely, children with high ventral attention connectivity exhibit functional organization that follows the typical pattern of brain maturation. The permutation analyses demonstrate that the amount of variance accounted for by the association cortex anchored gradient is increased in the low (Gradient 1 variance: 0.3648) relative to high ventral attention connectivity participants (Gradient 2 variance: 0.1052;  $P = 0$ , 0 of 500 permutations revealed greater difference than the real situation). Consistent with this profile, the amount of variance accounted for by the unimodal anchored gradient is decreased in the low (Gradient 2 variance: 0.1161) relative to high ventral attention connectivity participants (Gradient 1 variance: 0.3846;  $P = 0$ , 0 of 500 revealed greater difference than the real situation).

Conversely, in adolescence, we did not observe a significant difference between the high and low ventral attention groups in the first association cortex anchored gradient (0.3807 versus 0.3595;  $P = 0.0620$ ), whereas the second gradient in high ventral attention adolescent group (0.1052) accounted for a significantly lower amount of variance ( $P = 0.008$ , 4 in 500 permutations revealed lower difference than the real situation) than the low ventral attention adolescent group (0.1161).

The accelerated longitudinal design of the CCNP<sup>31,37</sup>, which includes longitudinal tracking data with a visiting interval of 1.25 years, provided for additional analyses in participants who were scanned both before (child group) and after their 12th birthday (adolescent group). Here, we identified a set of child participants ( $n = 22$ ) from the low ventral attention group who were also scanned subsequently in their adolescence ( $n = 26$ , mean age of initial scan =  $10.98 \pm 0.64$  years; mean age of second scan =  $12.90 \pm 0.69$  years). In the participants classified as low ventral attention in childhood, when they transition to adolescence, their first gradient in childhood is highly correlated ( $r = 0.9429$ ,  $P < 0.01$ ) with the first gradient that in their adolescence. A consistent group profile that was also evident when considering their second gradients in both childhood and adolescence ( $r = 0.9353$ ,  $P < 0.01$ ; Extended Data Fig. 2).

Conversely, high ventral attention children ( $n = 21$ ), who were also scanned in their adolescence ( $n = 24$ , mean age of initial scan =  $11.09 \pm 0.63$ ; mean age of second scan =  $12.94 \pm 0.71$ ), displayed a normative developmental trajectory. Here, their first gradient in childhood was highly correlated with their second gradient in adolescence (absolute  $r = 0.9793$ ,  $P < 0.01$ ), while their second gradient in childhood was highly correlated with the first gradient in their adolescence (absolute  $r = 0.9748$ ,  $P < 0.01$ ; Extended Data Fig. 3).

If the salience/ventral attention network contributes to the maturation of cortical hierarchy, the functional integrity of attentional systems may also associate with changes in cognitive and behavioral performance. To examine this hypothesis, we next assessed the relationship between standardized measures of cognitive functioning (IQ) and the degree centrality of the ventral attention network with an LME model. LME models for IQ subdomain scores in verbal, perceptual reasoning, working memory, processing speed and a composite total score were constructed separately. Age, gender, head motion and the vertex-level connectivity counts with ventral attention network were fed into each LME model as fixed effects, repeated measurements

were set as the random effect. Results revealed significant negative associations between ventral attention network connectivity and verbal ( $P \leq 0.05$ ), perceptual reasoning ( $P \leq 0.01$ ) and the composite IQ scores ( $P \leq 0.05$ ). Associations with participant age and verbal score ( $P \leq 8 \times 10^{-6}$ ), perceptual reasoning score ( $P \leq 0.05$ ) and total score ( $P \leq 0.001$ ), as well as associations with gender and verbal score ( $P \leq 0.05$ ), perceptual reasoning score ( $P \leq 0.05$ ) and total score ( $P \leq 0.05$ ) were also observed. Suggesting that this pattern was not due to variability in data quality, no significant associations between IQ scores and head motion were evident ( $P > 0.05$ ; see LME results in Supplementary Tables 3–7 for each IQ subdomain score).

Collectively, these results demonstrate that individual variability within the attention network in children associates with dissociable motifs of connectivity across the functional connectome and covaries with cognitive functioning. Children with low ventral attention connectivity exhibit an accelerated profile of cortical maturation that closely resembles previous reports in adolescents and adults. Although additional longitudinal analyses are warranted, these data suggest a fundamental relationship between individual variability within the ventral attention network and the age-dependent changes in the macroscale properties of human brain organization and cognitive ability.

### Ventral attention network connectivity reliably associates with accelerated cortical maturation and cognitive ability across populations

The analyses above reveal a relationship between ventral attention network connectivity, the functional maturation of the cortical connectome and cognitive functioning in a population of healthy developing children and adolescents from the CCNP<sup>31,37</sup>. To examine the generalizability of the above results, we utilized 2,186 participants from the adolescent brain cognitive development (ABCD)<sup>38</sup> study, where participant data differed from the CCNP in sample population, study site, magnetic resonance imaging (MRI) scanner, acquisition parameters and longitudinal designs. Here, the ABCD data were limited to participants between 9 and 11 years old. Highlighting the robustness of the analyses reported above, we observed a profile of heightened degree centrality in ventral attention network areas that was consistent with the CCNP analyses (Fig. 1a). Broadly, the ABCD degree centrality map demonstrated a lower degree centrality distribution along the cortex than the CCNP dataset (Fig. 5a). Here, the inferior parietal gyrus and supramarginal gyrus, together with middle anterior cingulate cortex exhibited highly connected architecture. Hub regions of default network including the angular gyrus, middle temporal gyrus and postcingulate cortex also revealed heightened degree centrality in the ABCD data, which might again indicate the role of default network as a critical cortical core across the transition to adolescence.

Next, we assessed the reliability of a relationship linking the maturation of functional gradient architecture of the cortical sheet with individual variability in ventral attention connectivity across populations. To do so, we split the children in the ABCD study in a manner consistent with the CCNP analyses to examine whether the ventral attention network connections are coupled with the functional gradient maturation. No significant associations were observed between the degree centrality of ventral attention network and demographic factors such as age ( $P = 0.21$ ), gender ( $P = 0.60$ ), head motion ( $P = 0.12$ ) and family income ( $P = 0.15$ ). Further comparisons reveal matched demographic features between child groups in age ( $P = 0.80$ ), gender ( $P = 0.39$ ), head motion ( $P = 0.51$ ) and family income ( $P = 0.15$ ). Consistent with our findings in the CCNP children group, the gradient profiles of children with high ventral attention network connectivity in the ABCD study ( $n = 1,367$ ) displayed the developmentally typical gradient profile (Fig. 4b). In this group, the primary visual and somato/motor areas occupied the ends of the primary gradient, matched the second gradients in CCNP adolescents ( $r = 0.896$ ,  $P_{\text{spin}} \leq 0.001$ ) and Human Connectome Project (HCP) adults ( $r = 0.93$ ,  $P_{\text{spin}} \leq 0.001$ ), whereas

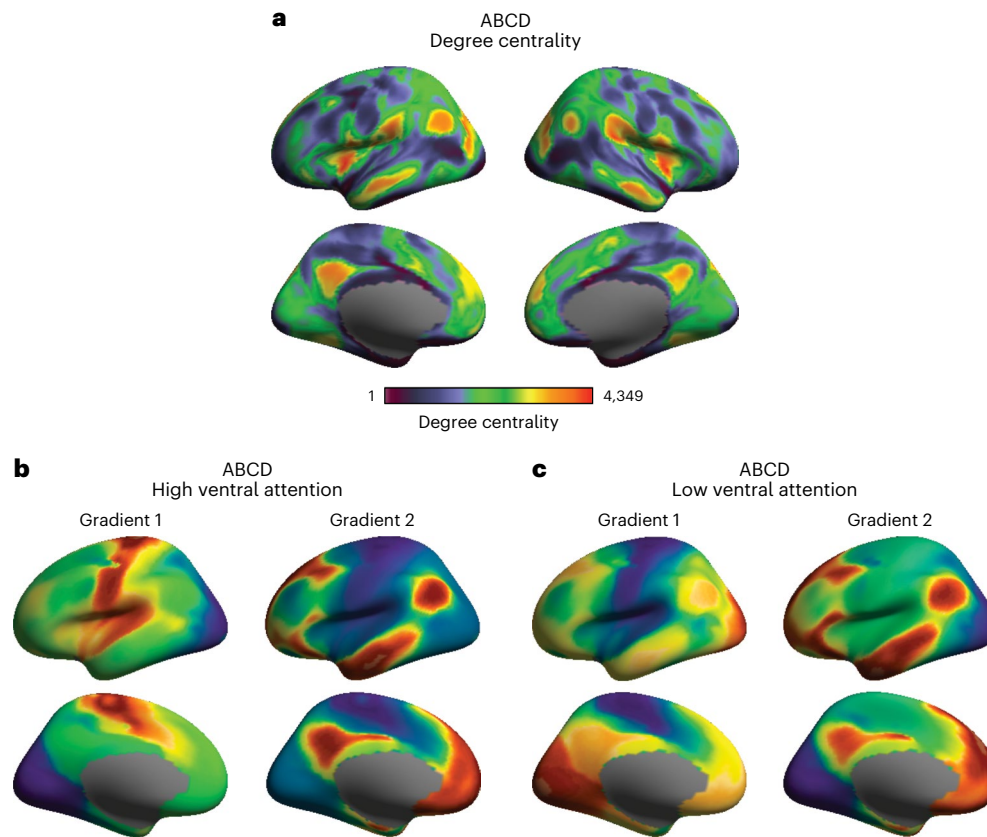


**Fig. 5 | Relationship between ventral attention network connectivity and accelerated cortical maturation is reliable across independent datasets.** **a**, Degree centrality maps in children (9–11 years old,  $n = 2,186$ ) from the ABCD project reveals dense connectivity in ventral attention network areas in a pattern that is consistent with the CCNP participants (Fig. 1a). Scale bar reflects the count of above-threshold connections from a given vertex compared with all other vertices. Larger values indicate higher degree centrality. **b**, Gradient

maps in the ABCD high ventral attention connectivity groups reveal typical patterns identified in our previous work in children<sup>14</sup> as well as the CCNP high ventral attention group (Fig. 4b,c children). **c**, Gradient maps in the ABCD low ventral attention connectivity groups closely resemble the profile of accelerated maturation observed in the CCNP sample. Here, the color scale represents the gradient values across the cortical surface. Vertices with similar colors indicate similarities in their functional connectome.

the second gradient revealed transmodal organization matching the first gradients in CCNP adolescents ( $r = 0.918$ ,  $P_{\text{spin}} \leq 0.001$ ) and HCP adults ( $r = 0.944$ ,  $P_{\text{spin}} \leq 0.001$ ). An accelerated developmental profile was revealed in the ABCD children with low ventral attention network links ( $n = 819$ ), broadly matching the primary and secondary gradients identified previously in CCNP adolescents (Gradient 1:  $r = 0.865$ ,  $P_{\text{spin}} \leq 0.001$ ; Gradient 2:  $r = 0.856$ ,  $P_{\text{spin}} \leq 0.001$ ) and demonstrating a hybrid organization comparing with HCP adults (correlations between the first gradient in ABCD low attention group and gradients in HCP adults:  $r = 0.61$ ,  $P_{\text{spin}} \leq 0.001$ ,  $r = 0.73$ ,  $P_{\text{spin}} \leq 0.001$ ; correlations between the second gradient in ABCD low attention group and gradients in HCP adults:  $r = 0.71$ ,  $P_{\text{spin}} \leq 0.001$ ,  $r = 0.62$ ,  $P_{\text{spin}} = 0.002$ ). These data provide converging evidence, across independent collection efforts, of an association between attention system connectivity and the broader functional organization and maturational properties of cortex.

As a final step, we repeated the behavior association analysis in the ABCD project. Here, National Institutes of Health (NIH) toolbox scores were used to access cognitive abilities, including crystallized (picture vocabulary and oral reading recognition) and fluid components (pattern comparison processing speed, list sorting working memory, picture sequence memory, flanker test and dimensional change card sort)<sup>39</sup>. As above, a linear regression model was conducted to examine the relationship between the degree centrality of the ventral attention network and cognitive functioning. Age, sex and head motion were set as covariates in the model. Consistent with our CCNP results, these analyses revealed that the functional connections of ventral attention

network were associated significantly with the cognition total composite standard score ( $P = 0.0024$ ), crystallized composite standard score ( $P = 0.022$ ), cognition fluid composite standard score ( $P = 0.0058$ ), picture vocabulary ( $P = 0.0048$ ) and list sorting working memory ( $P = 0.0025$ ). Other significant associations are reported in Supplementary Tables 1–17. Only the cognition total composite standard score ( $P = 0.0024$ ) and list sorting working memory ( $P = 0.0025$ ) in the ABCD dataset were significant after Bonferroni correction to address multiple comparisons across a total of 15 LME and linear regression models; no significant association was revealed in the CCNP dataset after correction.

The replication analysis in the ABCD dataset highlights a potentially key role for the ventral attention network in the maturation process of both cortical hierarchy and cognitive ability. Notably, speaking to the robustness of the observed results, the differences across datasets are quite substantial, including but not limited to participant race, ethnicity, culture and environment as well as scanner, scanning parameters, socioeconomic factors and education. In particular, the distinct ethnic/racial composition of study samples can impact the generalizability of brain–behavior associations<sup>40,41</sup>. Here, we applied the connection counts with ventral attention network derived from the CCNP dataset directly on the children in the ABCD dataset and revealed consistent findings. Across sample collections, children with high ventral attention network connectivity demonstrated typical developmental patterns in functional gradients, whereas those with lower relative connectivity exhibited adolescent- and adult-like gradients.



The degree centrality of the ventral attention network is associated significantly with similar cognitive components in the CCNP and ABCD datasets. Collectively, these analyses suggest a close and generalizable relationship between the ventral attention network and the process of cortical maturation, as reflected in the presence of macroscale functional gradients. These data are in line with the hypothesis that the ventral attention network may preferentially drive the refinement in the macroscale organization of cortex and cognitive ability during the transition from childhood to adolescence.

## Discussion

A fundamental goal of developmental systems neuroscience is to identify the mechanisms that underlie the scheduled emergence and maturation of the large-scale functional networks central to the information processing capabilities of the human brain. Previous work has demonstrated age-dependent shifts in macroscale organization of cortex<sup>6,9</sup>, revealing the presence of a dominant profile of unimodal cortical organization in children that is later replaced in adolescence by a distributed transmodal architecture spanning from unimodal regions through association cortex. In the current study, we further demonstrated that more connections were required in children to attain a transmodal dominant feature (Extended Data Fig. 1), indicating that diffuse connections across broad swaths of association cortex gradually replace the local connections in higher percentiles during adolescence. Although this sweeping developmental reorganization of network relationships across the cortical sheet coincides with the transition from childhood to adolescence, reflecting an inflection point at around age 12–14 years, the neurobiological processes underpinning these profound functional changes have yet to be established. Here, by first identifying the densely connected hub regions across development, we demonstrate that ventral attention network regions<sup>11</sup> encompassing aspects of anterior insula, mPFC, and dorsal anterior cingulate cortex/midline supplementary motor area (also see salience<sup>27</sup> and cingulo-opercular action-mode<sup>26</sup> networks) may be linked to age-dependent shifts in the macroscale organization of cortex across childhood and adolescence.

Although the attention regions identified in the present analyses are recognized as a single system at a coarse scale<sup>42,43</sup>, this broad architecture is comprised of several spatially adjacent but functionally dissociable networks<sup>11,26,27,44</sup>. This complex system is theorized to underpin a cascade of functions supporting information processing, from the control of stimulus-driven attention<sup>43</sup> to the initialization of task sets and maintenance of sustained attention during goal pursuit<sup>29</sup>. The salience/ventral attention network was proposed to have a causal effect on switching between default and frontoparietal networks during task execution<sup>45</sup>. The hierarchical flow of information from sensory regions to deeper levels of cortical processing is also reflected in the spatial continuity of associated functional parcels along the cortical surface, for example, the salience network<sup>25,27</sup>, spanning orbital fronto-insular and dorsal anterior cingulate areas through broad posterior areas of insula and dorsal anterior cingulate cortex<sup>25,29</sup>. Broadly, information propagates along posterior to anterior, as well as dorsal to ventral, axes across cortex and the associated organization of functionally linked parcels is reflected through the presence of continuous functional gradients<sup>10,14</sup>. Here, the ventral attention network is situated at an intermediate position along this functional spectrum, transiting from primary sensory/motor networks to the default network that anchors association cortex, which is commonly identified as the first gradient in adolescence and adulthood, while reflecting the second gradient in childhood<sup>14</sup>. This transmodal organizational profile has been inferred to reflect the hierarchy of information flow across cortical territories<sup>10</sup>. Converging evidence for this functional motif has been revealed through analyses of step-wise connectivity. Consistent with classic theories regarding the integration of perceptual modalities into deeper layers of cortical processing<sup>23</sup>, functional relationships spread

from primary somato/motor, visual and auditory cortex before converging within ventral attention territories, and eventually the default network<sup>24</sup>. As a whole, these data provide clear evidence situating the ventral attention network between primary unimodal and association cortices, highlighting a role for attention systems in the functional propagation of sensory information to the multimodal regions that support higher-order cognitive functions.

The cingulo-opercular/ventral attention network, together with frontoparietal network, have been proposed to constitute a parallel architecture of executive functioning and cognitive control, supporting adaptive goal pursuit and flexible behavioral adjustments<sup>28</sup>. Although the frontoparietal network, encompassing aspects of dorsolateral prefrontal, dorsomedial prefrontal, lateral parietal and posterior temporal cortices, is functionally dissociable from cingulo-opercular action-mode/ventral attention network in adulthood, studies in developmental populations have revealed that they are functionally linked before adolescence<sup>18</sup>. Moreover, in children, the ventral attention network possesses a broad distributed connectivity profile with reduced segregation from salience networks<sup>46</sup>, perhaps reflecting fluid community boundaries in those areas. Anterior prefrontal cortex is shared by the two networks in children but later segregated into ventral attention network in early adolescence, with dorsal anterior cingulate cortex incorporated into frontoparietal network in adulthood<sup>18</sup>. This aspect of network development is consistent with evidence for increased, but more diffuse, patterns of task-evoked activity in children relative to adults<sup>47</sup>, reflecting the presence of a scattered pattern of community assignments in prefrontal territories, particularly those supporting attentional processes<sup>22</sup>. Further analysis revealed that virtually lesioning the entire frontoparietal network in children also generates transmodal organization in the first gradient (Extended Data Fig. 4).

Suggesting a key role for the attentional systems in cognition, our present analyses revealed reliable associations between attention network connectivity and broad measures of intellectual functioning across populations. A recent study also revealed abnormal functioning within limbic and insular networks and associated cognitive deficits in adolescents who were extremely preterm at birth<sup>48</sup>. The maturational course of large-scale brain network coincides with the emergence of adult-like performance on cognitive tasks (for example, processing speed, shifting and response inhibition)<sup>49,50</sup>. A pattern of attention network development that is theorized to reflect a transition from the over-representation of bottom-up attention to greater top-down attentional and executive functioning capabilities<sup>46</sup>. Converging evidence indicates that ventral attention network functions are intricately linked with the frontoparietal network in both anatomy and function. Although speculative, the corresponding segregation and integration of associated processes probably underpins the maturation of adaptive human cognition.

In the present data, the observed maturational changes were not distributed uniformly across cortical surface, suggesting a key role for the ventral attention network during development. Intriguingly, the greatest functional changes were not evident within the default or primary sensory territories that anchor the functional gradients in adolescence and adulthood. Rather, ventral attention and frontoparietal networks reflected the predominate sources of functional variation across childhood and adolescence (Fig. 1e). Of note, developmental changes were not exclusive to attentional network regions; the default network and the somato/motor network also demonstrated age-related variations across childhood and adolescence. These data are consistent with previous reports suggesting that somato/motor and ventral attention networks are functionally coupled in children, highlighting a distinct community architecture in children relative to adults<sup>22</sup>. Even in adulthood, the ventral areas in somato/motor network can be identified as a separate cluster from dorsal areas as network parcellations increase in their granularity (that is, 7-network relative to 17-network resolutions in Ye et al.<sup>11</sup> or in Gordon et al.,<sup>44</sup>).

Previous work has revealed a dramatic developmental change in the topography of ventral attention network, while the spatial organization of default network approaches an adult-like form in childhood<sup>22</sup>. However, it should be noted that the developmental changes in brain's functional hierarchy are driven by comprehensive reconfigurations across broad swaths of cortex, rather than reflecting solely developmentally mediated shifts in the ventral attention network alone. As illustrated in Fig. 3, there are substantial alterations in both between- and within-network connections across different age groups. This is particularly evident in the default network, where a profile of age-linked increases in within-network connectivity replaced between-network connections. These extensive changes along the cortical surface indicate that network organization is not stabilized during development, raising the critical issue of whether a given cortical area belongs to a fixed network across puberty and into adulthood. Future studies should further establish an accurate network affiliation for the developing population. Of note, the size and shape of the human brain undergoes substantial changes throughout the lifespan. While it is indicated that the growth velocities of brain tissues peak before 6 years old<sup>9</sup>, caution is essential when interpreting MRI studies that span development populations. Factors such as head motion and registration errors might bias the results. Therefore, validating with large, independent datasets and alternate methods of assessing brain functioning is crucial to assess the reproducibility, robustness and generalizability of the current results.

To further characterize how changes in ventral attention network connectivity might underlie the broad functional maturation of cortex, we directly excluded the developmentally dissociable aspects of ventral attention network from the brain connectome and rederived the functional gradients previously characterized in children, adolescence<sup>14</sup> and adults<sup>10</sup>. The present analyses revealed that virtually lesioning ventral attention clusters characterized by the greatest developmental changes generates adolescent- and adult-like gradient architectures in children—a profile that was specific to attention network territories. Although follow-up work is necessary, our analyses are consistent with the presence of a relative increase in local connections between ventral attention network and adjacent somato/motor territories in childhood, biasing a functional motif in childhood dominated by unimodal organization. Later, diffuse connections across broad swaths of association cortex emerge with age, until eventually the presence of interactions across distinct systems becomes the dominant feature of cortical organization. The increased emphasis on such transmodal integration is consistent with the developmental principle that, over time, local connections are replaced by remote distributed interactions<sup>13</sup>.

Individual level analysis further reveals the influence of ventral attention network on the formation of adult-like functional organization. Children with fewer ventral attention network connections exhibited an accelerated transmodal profile of cortical organization, while the typical unimodal dominated architecture was presented in children with more ventral attention connections. However, an open unanswered question remains the manner through which ventral attention network functioning may reshape the macroscale organization of the cortex. Although speculative, the observed results might reflect a consequence of repeated coactivation between ventral attention network regions and associated cortical systems<sup>18</sup>. Accordingly, the dense associations with somato/motor areas<sup>22</sup> as well as frontoparietal areas<sup>18</sup> in children indicates ventral attention or action-mode network<sup>51</sup> is connected preferentially by both primary and association cortex during development, which is also evident in our degree centrality map (Fig. 1a,b). Although a dense profile of connections may ensure system integrity, excessive or redundant connections are pruned across development to optimize efficient information processing as neurons that are not fully integrated within local circuits are eliminated to ensure stable network function<sup>52</sup>. A profile of network segregation and integration that is hypothesized to underpin functional specialization and computational efficiency<sup>19,53</sup>.

Along with the stabilization of its functional organization, cortical maturation is also marked by increased flexibility in resource allocation during task execution. Evidence from task-based functional MRI (fMRI) suggests that the salience/ventral attention network, especially the right fronto-insular cortex, plays a critical role in switching between the default and frontoparietal networks<sup>45</sup>. This finding supports our hypothesis that the ventral attention network serves not only as a transfer hub between unimodal and transmodal cortices but also coordinates the information flow within the transmodal cortex. In addition to refining the unstable local connections associated with unimodal areas, the ventral attention network may drive the predominance of transmodal organization through a parallel mechanism, which likely involves strengthening the transmodal interactions among higher-order networks to ensure the flexible reallocation of resources. Future work should focus on characterizing the specific properties of ventral attention network across development, for instance, extending to early points in the lifespan, examining its interactions with other networks under the background of task execution, or considering the role of individual experience on network development<sup>54,55</sup>.

Accumulating evidence has revealed a dramatic restructuring of the macroscale organization of the cortex across development, suggesting the scheduled maturation of functional gradient patterns may be critically important for understanding how cognitive and behavioral capabilities are refined across development. However, the underlying developmental processes driving these functional changes remain to be established. Here, by first localizing the significant maturational changes in functional connectome across childhood and adolescence, we demonstrate that the ventral attention network may play a critical role in the onset of the age-dependent shifts that characterize the macroscale organization of cortex across development. Children with fewer functional connections within the ventral attention network exhibit the appearance of an accelerated maturation of gradient architecture and increased cognitive functioning. Although the process of brain maturation emerges through complex interactions across environmental experience and biological systems that span genes and molecules through cells, networks and behavior, the current findings suggest a core role for attention network-linked territories. The multiscale interactions linking the longitudinal development of the ventral attention network with these maturational processes, and the associated consequences on behavior across health and disease, remains an open question to be answered in future work.

## Online content

Any methods, additional references, Nature Portfolio reporting summaries, source data, extended data, supplementary information, acknowledgements, peer review information; details of author contributions and competing interests; and statements of data and code availability are available at <https://doi.org/10.1038/s41593-024-01736-x>.

## References

1. Casey, B. J., Heller, A. S., Gee, D. G. & Cohen, A. O. Development of the emotional brain. *Neurosci. Lett.* **693**, 29–34 (2019).
2. Casey, B. J., Getz, S. & Galvan, A. The adolescent brain. *Dev. Rev.* **28**, 62–77 (2008).
3. Luna, B. et al. Maturation of widely distributed brain function subserves cognitive development. *Neuroimage* **13**, 786–793 (2001).
4. Kang, H. J. et al. Spatio-temporal transcriptome of the human brain. *Nature* **478**, 483–489 (2011).
5. Huttenlocher, P. R. & Dabholkar, A. S. Regional differences in synaptogenesis in human cerebral cortex. *J. Comp. Neurol.* **387**, 167–178 (1997).
6. Paquola, C. et al. Shifts in myeloarchitecture characterise adolescent development of cortical gradients. *eLife* **8**, e50482 (2019).

7. Zilles, K., Palomero-Gallagher, N. & Amunts, K. Development of cortical folding during evolution and ontogeny. *Trends Neurosci.* **36**, 275–284 (2013).
8. Reardon, P. K. et al. Normative brain size variation and brain shape diversity in humans. *Science* **360**, 1222–1227 (2018).
9. Bethlehem, R. A. I. et al. Brain charts for the human lifespan. *Nature* **604**, 525–533 (2022).
10. Margulies, D. S. et al. Situating the default-mode network along a principal gradient of macroscale cortical organization. *Proc. Natl Acad. Sci. USA* **113**, 12574–12579 (2016).
11. Yeo, B. T. et al. The organization of the human cerebral cortex estimated by intrinsic functional connectivity. *J. Neurophysiol.* **106**, 1125–1165 (2011).
12. Gao, W. et al. Temporal and spatial evolution of brain network topology during the first two years of life. *PLoS ONE* **6**, e25278 (2011).
13. Fair, D. A. et al. Functional brain networks develop from a ‘Local to Distributed’ organization. *PLoS Comput. Biol.* **5**, e1000381 (2009).
14. Dong, H. M., Margulies, D. S., Zuo, X. N. & Holmes, A. J. Shifting gradients of macroscale cortical organization mark the transition from childhood to adolescence. *Proc. Natl Acad. Sci. USA* **118**, e2024448118 (2021).
15. Somerville, L. H., Hare, T. & Casey, B. J. Frontostriatal maturation predicts cognitive control failure to appetitive cues in adolescents. *J. Cogn. Neurosci.* **23**, 2123–2134 (2011).
16. Tottenham, N. & Sheridan, M. A. A review of adversity, the amygdala and the hippocampus: a consideration of developmental timing. *Front. Hum. Neurosci.* **3**, 68 (2009).
17. Sydnor, V. J. et al. Neurodevelopment of the association cortices: patterns, mechanisms, and implications for psychopathology. *Neuron* **109**, 2820–2846 (2021).
18. Fair, D. A. et al. Development of distinct control networks through segregation and integration. *Proc. Natl Acad. Sci. USA* **104**, 13507–13512 (2007).
19. Betzel, R. F. et al. Changes in structural and functional connectivity among resting-state networks across the human lifespan. *Neuroimage* **102**, 345–357 (2014).
20. Betzel, R. F. et al. Generative models of the human connectome. *Neuroimage* **124**, 1054–1064 (2016).
21. Zuo, X. N. et al. Human connectomics across the life span. *Trends Cogn. Sci.* **21**, 32–45 (2017).
22. Tooley, U. A., Bassett, D. S. & Mackey, A. P. Functional brain network community structure in childhood: Unfinished territories and fuzzy boundaries. *Neuroimage* **247**, 118843 (2022).
23. Mesulam, M. M. From sensation to cognition. *Brain* **121**, 1013–1052 (1998).
24. Sepulcre, J., Sabuncu, M. R., Yeo, T. B., Liu, H. & Johnson, K. A. Stepwise connectivity of the modal cortex reveals the multimodal organization of the human brain. *J. Neurosci.* **32**, 10649–10661 (2012).
25. Power, J. D. et al. Functional network organization of the human brain. *Neuron* **72**, 665–678 (2011).
26. Dosenbach, N. U. et al. Distinct brain networks for adaptive and stable task control in humans. *Proc. Natl Acad. Sci. USA* **104**, 11073–11078 (2007).
27. Seeley, W. W. et al. Dissociable intrinsic connectivity networks for salience processing and executive control. *J. Neurosci.* **27**, 2349–2356 (2007).
28. Dosenbach, N. U., Fair, D. A., Cohen, A. L., Schlaggar, B. L. & Petersen, S. E. A dual-networks architecture of top-down control. *Trends Cogn. Sci.* **12**, 99–105 (2008).
29. Dosenbach, N. U. et al. A core system for the implementation of task sets. *Neuron* **50**, 799–812 (2006).
30. Labache, L., Ge, T., Yeo, B. T. T. & Holmes, A. J. Language network lateralization is reflected throughout the macroscale functional organization of cortex. *Nat. Commun.* **14**, 3405 (2023).
31. Liu, S. et al. Chinese color nest project: an accelerated longitudinal brain-mind cohort. *Dev. Cogn. Neurosci.* **52**, 101020 (2021).
32. Alexander-Bloch, A. F. et al. On testing for spatial correspondence between maps of human brain structure and function. *Neuroimage* **178**, 540–551 (2018).
33. Schaefer, A. et al. Local-global parcellation of the human cerebral cortex from intrinsic functional connectivity MRI. *Cereb. Cortex* **28**, 3095–3114 (2018).
34. Gogtay, N. et al. Dynamic mapping of human cortical development during childhood through early adulthood. *Proc. Natl Acad. Sci. USA* **101**, 8174–8179 (2004).
35. Langs, G. et al. Identifying shared brain networks in individuals by decoupling functional and anatomical variability. *Cereb. Cortex* **26**, 4004–4014 (2016).
36. Coifman, R. R. & Lafon, S. Diffusion maps. *Appl. Comput. Harmon. A* **21**, 5–30 (2006).
37. Fan, X. R. et al. A longitudinal resource for population neuroscience of school-age children and adolescents in China. *Sci. Data* **10**, 545 (2023).
38. Casey, B. J. et al. The Adolescent Brain Cognitive Development (ABCD) study: imaging acquisition across 21 sites. *Dev. Cogn. Neurosci.* **32**, 43–54 (2018).
39. Luciana, M. et al. Adolescent neurocognitive development and impacts of substance use: overview of the adolescent brain cognitive development (ABCD) baseline neurocognition battery. *Dev. Cogn. Neurosci.* **32**, 67–79 (2018).
40. Ricard, J. A. et al. Confronting racially exclusionary practices in the acquisition and analyses of neuroimaging data. *Nat. Neurosci.* **26**, 4–11 (2023).
41. Li, J. et al. Cross-ethnicity/race generalization failure of behavioral prediction from resting-state functional connectivity. *Sci. Adv.* **8**, eabj1812 (2022).
42. Fox, M. D. et al. The human brain is intrinsically organized into dynamic, anticorrelated functional networks. *Proc. Natl Acad. Sci. USA* **102**, 9673–9678 (2005).
43. Corbetta, M. & Shulman, G. L. Control of goal-directed and stimulus-driven attention in the brain. *Nat. Rev. Neurosci.* **3**, 201–215 (2002).
44. Gordon, E. M. et al. Precision functional mapping of individual human brains. *Neuron* **95**, 791–807 e797 (2017).
45. Sridharan, D., Levitin, D. J. & Menon, V. A critical role for the right fronto-insular cortex in switching between central-executive and default-mode networks. *Proc. Natl Acad. Sci. USA* **105**, 12569–12574 (2008).
46. Farrant, K. & Uddin, L. Q. Asymmetric development of dorsal and ventral attention networks in the human brain. *Dev. Cogn. Neurosci.* **12**, 165–174 (2015).
47. Casey, B. J., Giedd, J. N. & Thomas, K. M. Structural and functional brain development and its relation to cognitive development. *Biol. Psychol.* **54**, 241–257 (2000).
48. Molloy, M. F. et al. Effect of extremely preterm birth on adolescent brain network organization. *Brain Connect.* **13**, 394–409 (2023).
49. Huizinga, M., Dolan, C. V. & van der Molen, M. W. Age-related change in executive function: developmental trends and a latent variable analysis. *Neuropsychologia* **44**, 2017–2036 (2006).
50. Luna, B., Garver, K. E., Urban, T. A., Lazar, N. A. & Sweeney, J. A. Maturation of cognitive processes from late childhood to adulthood. *Child Dev.* **75**, 1357–1372 (2004).
51. Gordon, E. M. et al. A somato-cognitive action network alternates with effector regions in motor cortex. *Nature* **617**, 351–359 (2023).



52. Pfisterer, U. & Khodosevich, K. Neuronal survival in the brain: neuron type-specific mechanisms. *Cell Death Dis.* **8**, e2643 (2017).
53. Bullmore, E. & Sporns, O. The economy of brain network organization. *Nat. Rev. Neurosci.* **13**, 336–349 (2012).
54. Gee, D. G. et al. Early developmental emergence of human amygdala-prefrontal connectivity after maternal deprivation. *Proc. Natl Acad. Sci. USA* **110**, 15638–15643 (2013).
55. Dong, H. M. et al. Charting brain growth in tandem with brain templates at school age. *Sci. Bull.* **65**, 1924–1934 (2020).

**Publisher's note** Springer Nature remains neutral with regard to jurisdictional claims in published maps and institutional affiliations.

Springer Nature or its licensor (e.g. a society or other partner) holds exclusive rights to this article under a publishing agreement with the author(s) or other rightsholder(s); author self-archiving of the accepted manuscript version of this article is solely governed by the terms of such publishing agreement and applicable law.

© The Author(s), under exclusive licence to Springer Nature America, Inc. 2024

## Methods

### Datasets

**Chinese color nest project.** CCNP is a 5-year accelerated longitudinal study across the human lifespan<sup>21,31,37,56</sup>. A total of 176 scans in adolescents and 202 scans in typically developing children were included in the analysis; details of the dataset and exclusion criteria can be found in our previous work<sup>14</sup>. All MRI data were obtained with a Siemens Trio 3.0 T scanner at the Faculty of Psychology, Southwest University in Chongqing. The reported experiments were approved by the Institutional Review Board from Institute of Psychology, Chinese Academy of Sciences. All participants and their parents/guardians provided written informed consent before participating in the study.

**ABCD study.** ABCD is a multisite longitudinal cohort following the brain and cognition development of over 10,000 children aged 9–10 years. MRI scans including T1-weighted, T2-weighted and resting-state fMRI was obtained with 3 T Siemens Prisma, General Electric 750 and Phillips scanners across 21 sites; details of the scan parameters can be found in ref.5. Here, we unitized the MRI baseline data from 2,186 children (female participants, 54.4%; mean age 10.01 years) for the reproducibility analysis. The study was approved by the Institutional Review Board from the University of California, San Diego<sup>57</sup>. All participants and their parents/guardians provided written informed consent<sup>58</sup>.

### MRI data preprocessing

**CCNP dataset.** Anatomical T1 images were inspected visually to exclude individuals with substantial head motion and structural abnormalities. Next, T1 images were fed into the volBrain pipeline (<https://volbrain.net/>)<sup>59</sup> for noise removal, bias correction, intensity normalization and brain extraction. All brain extractions underwent visual inspection to ensure tissue integrity. After initial quality checks, T1 images were passed into the connectome computation system<sup>60,61</sup> for surface-based analyses. The connectome computation system pipeline is designed for preprocessing multimodal MRI datasets and integrates publicly available software including SPM<sup>62</sup>, FSL<sup>63</sup>, AFNI<sup>64</sup> and FreeSurfer<sup>65</sup>. Resting-state fMRI data preprocessing included a series of steps common to intrinsic FC analyses: (1) dropping the first 10 s (four repetition times) for equilibrium of the magnetic field; (2) estimating head motion parameters and head motion correction; (3) slicing time correction; (4) timeseries despiking; (5) registering functional images to high resolution T1 images using boundary-based registration; (6) removing nuisance factors such as head motion, cerebrospinal fluid (CSF) and white matter signals using ICA-AROMA<sup>66</sup>; (7) removing linear and quadratic trends of the timeseries; (8) projecting volumetric timeseries to surface space (the fsaverage5 model with medial wall masked out); and (9) 6 mm spatial smoothing. All preprocessing scripts are publicly available on GitHub (<https://github.com/zuoxinian/CCS>). Any resting-state scan with a mean head motion above 0.5 mm was excluded from further analysis. The demographic information of subjects included in the analyses is listed in Supplementary Table 1.

**ABCD dataset.** Minimally preprocessed T1 images<sup>67</sup> were fed into FreeSurfer<sup>62</sup> for surface reconstruction. Resting-state fMRI data<sup>67</sup> preprocessing included a series of steps as following: (1) dropping the initial frames for equilibrium of the magnetic field; (2) estimating head motion parameters and voxel-wise differentiated signal variance and head motion correction; (3) registering functional images to high resolution T1 images using boundary-based registration; (4) scrubbing the frames with framewise displacement > 0.3 mm or voxel-wise differentiated signal variance > 50, along with one volume before and two volumes after; (5) removing nuisance factors such as global signal, head motion, CSF and white matter signals; (6) band-pass filtered ( $0.009 \text{ Hz} \leq f \leq 0.08 \text{ Hz}$ ); (7) projecting volumetric timeseries to surface space (the fsaverage5 model with medial wall masked out); and (8) 6 mm spatial smoothing. Full details of data preprocessing can be

found in a previous study<sup>68</sup>. All preprocessing scripts are publicly available ([https://github.com/ThomasYeoLab/ABCD\\_scripts](https://github.com/ThomasYeoLab/ABCD_scripts)) on GitHub. Any resting-state scan with a maximum head motion above 5 mm and over half of their volumes censored was excluded from further analysis.

### Degree centrality mapping

FC matrices and the corresponding Fisher-z transformed values were first generated for each resting-scan per visit. The two test-retest FC Fisher-z (FCz) matrices within one visit were averaged to increase signal-to-noise ratio for generating the individual FCz matrix for each visit, which was later averaged across individuals to form group-level FCz matrices. For the group-level FCz matrices, only the top 10% FCs of each vertex were retained, other elements and negative FCs in the matrix were set to 0 to enforce sparsity, yielding an asymmetrical matrix, the rows of which correspond to the connectome of each vertex. A degree centrality map was obtained by counting the nonzero elements in each column of the FCz matrix. We then calculated the cosine distance between any two rows of the FCz matrix and subtracted from 1 to obtain a symmetrical similarity matrix; this similarity matrix was later used to derive the gradients.

### Euclidean distance

To characterize the developmental changes between children and adolescents, the Euclidean distance was computed for each row of the cosine distance matrix between children and adolescents. The most changed clusters were then extracted according to the following two criteria: the top 10% in Euclidean distance map and the cluster size above 500 vertices. One-way analyses of variance were performed to test the statistical differences between networks.

### Gradients analysis

The extracted clusters and their FCs were first dropped in the initial FCz matrix of the child group, and the cosine similarity matrix was then calculated. Diffusion map embedding<sup>10,35</sup> was implemented on the similarity matrix to derive gradients ([https://github.com/NeuroanatomyAndConnectivity/gradient\\_analysis](https://github.com/NeuroanatomyAndConnectivity/gradient_analysis)). Within each age bin, the FC matrix from participants with repeated imaging scans was averaged with scans of other participants to generate a group-level matrix, and then used to derive functional gradients. Pearson correlations were computed between the derived gradients in children and adults. To examine the statistical significance of the observed Pearson correlations, null distributions were generated by randomly rotating the locations of the extracted clusters across the cortical surface while keeping the shape and size fixed. For each permutation, the gradients and correlations were rederived. A total of 500 permutations were performed to generate the null model.

### Chord diagram

A chord diagram was utilized to demonstrate the differences in numbers of FC between children and adolescents at network level. For each vertex, its connectome was represented as the corresponding row in the FCz matrix. The associated number of network-level connections was obtained by counting the nonzero elements in each network according to the Yeo seven-network solution, generating a matrix with dimension 20,484 (number of vertex) by seven (number of networks). Vertices were grouped into networks to generate the final network-to-network FC matrix (seven by seven). The rows of this network-to-network matrix are displayed as the links from right half circus with larger radius to the left smaller half circus, referring to the FCs with networks in its own connectome, the opposite links from left to right circus represent the columns in the network-to-network matrix, referring to the FCs of each network that were existed in other networks' connectome (Fig. 3).

### High and low ventral attention network group definition

Ventral attention network-linked connections were extracted as the corresponding column in network-to-network matrix, referring to the FC other networks linked with ventral attention network. As we found in

previous work<sup>14</sup>, gradient maps became stable in 15-year-old participants, although they still possess a hybrid organization relative to adult participants. The gradient pattern in 17-year-old participants closely resembles what is observed in adults. As such, we hypothesized that the functional connections may reach a stable status at the end of adolescence when compared with younger participants; thus, we take the median value of FC number in 17-year-old age group as the reference. Any single scan with a connectivity number above the threshold was assigned to the ‘high’ ventral attention subgroup, other scans were assigned to the ‘low’ ventral attention group. The gradients were then rederived for each group.

### Association analysis with IQ score in the CCNP dataset

The association between connections number with ventral attention network and IQ scores was estimated with LME model. IQ scores were obtained by Wechsler Children Intelligence Scale IV, including scores in following subdomains: verbal, perception reasoning, working memory and processing speed ability. The LME was conducted using the following formula:

$$\text{IQ\_score} \approx 1 + \text{age} + \text{gender} + (\text{ventral attention})_{\text{DC}} + \text{headmotion} + (1|\text{Subid})$$

Here (ventral attention)<sub>DC</sub> refers to the connections with ventral attention network, together with age, gender, head motion and the intercept set as the fixed effect factor. Subid refers to the participant IDs, multimeasurements for a single participant were coded as an identical nominal variable, set as the random effect factor. LME models were applied for the total IQ and subdomain scores separately.

### Association analysis with cognitive score in the ABCD dataset

Linear regression model was applied to estimate the association between connections number with ventral attention network and cognitive scores in the ABCD dataset. Cognitive scores were accessed by NIH toolbox, including scores in following domains: crystallized (picture vocabulary and oral reading recognition) and fluid components (pattern comparison processing speed, list sorting working memory, picture sequence memory, flanker test and dimensional change card sort)<sup>10</sup>. The model was conducted using the following formula in MATLAB:

$$\text{Cognitive\_score} \approx 1 + \text{age} + \text{gender} + (\text{ventral attention})_{\text{DC}} + \text{headmotion}$$

### Developmental effects on degree centrality of ventral attention network

The association between connections number with ventral attention network and age, gender head motion was also estimated with LME model, which was conducted using the following formula in MATLAB:

$$(\text{Ventral attention})_{\text{DC}} \approx 1 + \text{age} + \text{gender} + \text{headmotion} + (1|\text{Subid})$$

### Reporting summary

Further information on research design is available in the Nature Portfolio Reporting Summary linked to this article.

### Data availability

Data from the CCNP dataset used here are available at CCNP–Lifespan Brain-Mind Development Data Community at Science Data Bank (<https://ccnp.scidb.cn/en>) including both anonymized neuroimaging data (<https://doi.org/10.57760/sciencedb.07860>) and unthresholded whole-brain connectivity matrices grouped by relevant ages (children and adolescents) (<https://doi.org/10.11922/sciencedb.00886>). The raw CCNP data are available from the website upon reasonable request.

The ABCD data used in this report came from the Annual Release v.2.0 (<https://doi.org/10.15154/1503209>) of the ABCD BIDS Community Collection (ABCC; NDA Collection 3165). Source data are provided with this paper.

### Code availability

Code is available via GitHub: (1) preprocessing CCNP datasets (<https://github.com/zuoxinian/CCS>); (2) preprocessing ABCD datasets ([https://github.com/ThomasYeoLab/ABCD\\_scripts](https://github.com/ThomasYeoLab/ABCD_scripts)); (3) FC gradient analysis ([https://github.com/NeuroanatomyAndConnectivity/gradient\\_analysis](https://github.com/NeuroanatomyAndConnectivity/gradient_analysis)); and (4) Gradient maturation analysis (<https://github.com/HolmesLab/GradientMaturation>).

### References

- Yang, N. et al. Chinese color nest project: growing up in China (in Chinese). *Chin. Sci. Bull.* **62**, 3008–3022 (2017).
- Auchter, A. M. et al. A description of the ABCD organizational structure and communication framework. *Dev Cogn Neurosci* **32**, 8–15 (2018).
- Clark, D. B. et al. Biomedical ethics and clinical oversight in multisite observational neuroimaging studies with children and adolescents: the ABCD experience. *Dev. Cogn. Neurosci.* **32**, 143–154 (2018).
- Manjon, J. V. & Coupe, P. volBrain: an online MRI brain volumetry system. *Front. Neuroinform.* **10**, 30 (2016).
- Xu, T. et al. A connectome computation system for discovery science of brain. *Sci. Bull.* **60**, 86–95 (2015).
- Xing, X. X. et al. Connectome computation system: 2015–2021 updates. *Sci. Bull.* **67**, 448–451 (2022).
- Friston, K. J. et al. Statistical parametric maps in functional imaging: a general linear approach. *Hum. Brain Mapp.* **2**, 189–210 (1994).
- Jenkinson, M., Beckmann, C. F., Behrens, T. E., Woolrich, M. W. & Smith, S. M. FSL. *Neuroimage* **62**, 782–790 (2012).
- Cox, R. W. AFNI: software for analysis and visualization of functional magnetic resonance neuroimages. *Comput. Biomed. Res.* **29**, 162–173 (1996).
- Fischl, B. FreeSurfer. *Neuroimage* **62**, 774–781 (2012).
- Pruim, R. H. R. et al. ICA-AROMA: a robust ICA-based strategy for removing motion artifacts from fMRI data. *Neuroimage* **112**, 267–277 (2015).
- Hagler, D. J. Jr. et al. Image processing and analysis methods for the adolescent brain cognitive development study. *Neuroimage* **202**, 116091 (2019).
- Chen, J. et al. Shared and unique brain network features predict cognitive, personality, and mental health scores in the ABCD study. *Nat. Commun.* **13**, 2217 (2022).

### Acknowledgements

This work was supported by the STI 2030—the major projects of the Brain Science and Brain-Inspired Intelligence Technology (2021ZD0200500 to X.-N.Z.), the National Institute of Mental Health (grants R01MH120080 and R01MH123245 to A.J.H.), the Major Fund for International Collaboration of National Natural Science Foundation of China (81220108014 to X.-N.Z.) and the National Basic Science Data Center ‘Interdisciplinary Brain Database for In vivo Population Imaging’ (ID-BRAIN to X.-N.Z.). B.T.T.Y. is supported by the NUS Yong Loo Lin School of Medicine (NUHSRO/2020/124/TMR/LOA), the Singapore National Medical Research Council (NMRC) LCG (OFLCG19May-0035), NMRC CTG-IIT (CTGIIT23jan-0001), NMRC STaR (STaR20nov-0003), Singapore Ministry of Health (MOH) Centre Grant (CG21APR1009), the Temasek Foundation (TF2223-IMH-01) and the United States NIH (R01MH120080 and R01MH133334). Any opinions, findings and conclusions or recommendations expressed in this material are those of the authors and do not reflect the views of the Singapore NMRC, MOH or Temasek Foundation.



### Author contributions

H.-M.D., A.J.H. and X.-N.Z. designed the research. A.J.H. and X.-N.Z. supervised the research. H.-M.D. and A.J.H. conducted analyses and made figures. X.-H.Z., L.L., S.Z., L.Q.R.O. and B.T.T.Y. conducted validation analyses based on the ABCD dataset. H.-M.D., A.J.H. and X.-N.Z. wrote the initial draft. X.-H.Z., L.L., S.Z., L.Q.R.O., B.T.T.Y. and D.S.M. edited the paper.

### Competing interests

The authors declare no competing interests.

### Additional information

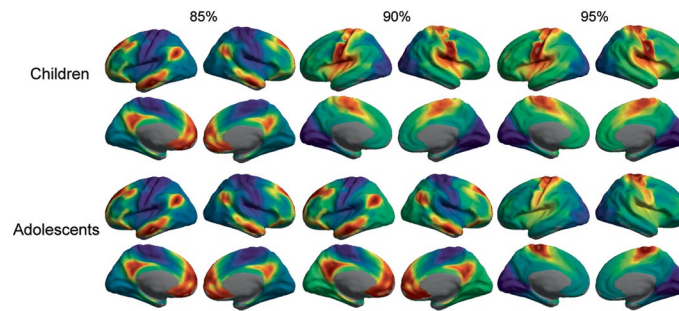
**Extended data** is available for this paper at <https://doi.org/10.1038/s41593-024-01736-x>.

**Supplementary information** The online version contains supplementary material available at <https://doi.org/10.1038/s41593-024-01736-x>.

**Correspondence and requests for materials** should be addressed to Hao-Ming Dong, Avram J. Holmes or Xi-Nian Zuo.

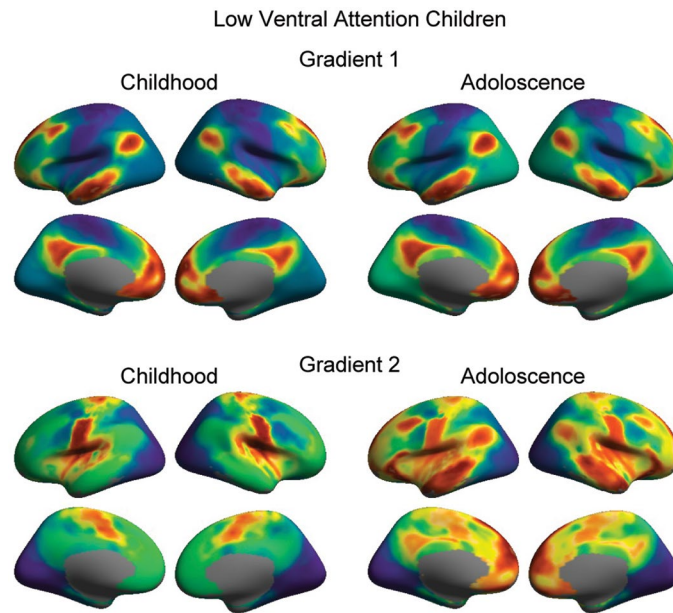
**Peer review information** *Nature Neuroscience* thanks Brenden Tervo-Clemmens and the other, anonymous, reviewer(s) for their contribution to the peer review of this work.

**Reprints and permissions information** is available at [www.nature.com/reprints](http://www.nature.com/reprints).



**Extended Data Fig. 1 | The transition from unimodal to transmodal organization revealed by the increasing in percentiles of functional connectome.** The threshold of connectivity matrices was adjusted in children and adolescent group and then redrive the gradients. The results revealed a marked transition in functional connectivity strength from childhood to adolescence. With the 95% threshold retaining the strongest connections, a unimodal organization was evident in both children and adolescents as their

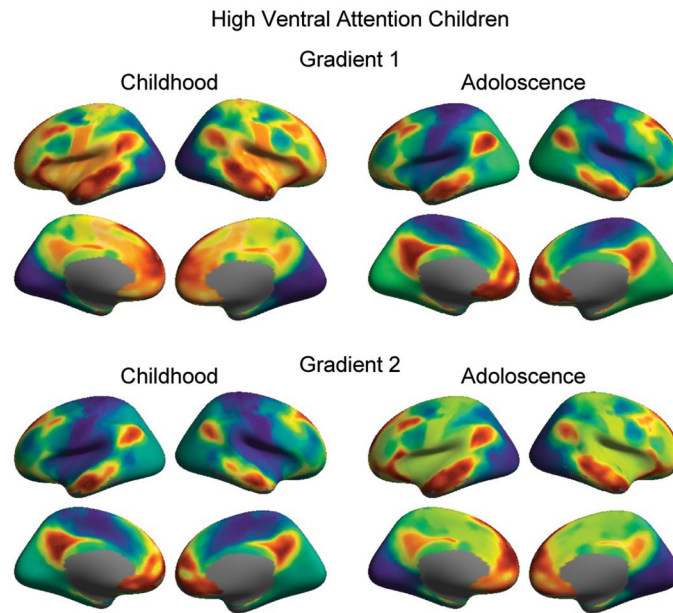
primary gradients. However, as additional weaker connections are included in the functional connectome at a 90% threshold, the primary gradients diverged for children and adolescents, revealing a unimodal and transmodal organization, respectively. Yet, with an 85% threshold incorporating even more weaker connections, the primary gradients converged into a transmodal organization for both children and adolescents.



**Extended Data Fig. 2 | Gradient maps in low ventral attention connectivity groups derived from longitudinal data.** A set of child participants ( $n=22$ ) were identified from the low ventral attention group who were also subsequently scanned in their adolescence. Surface maps exhibit a stable adolescent-like gradient architecture in both childhood and adolescence. Their first gradient

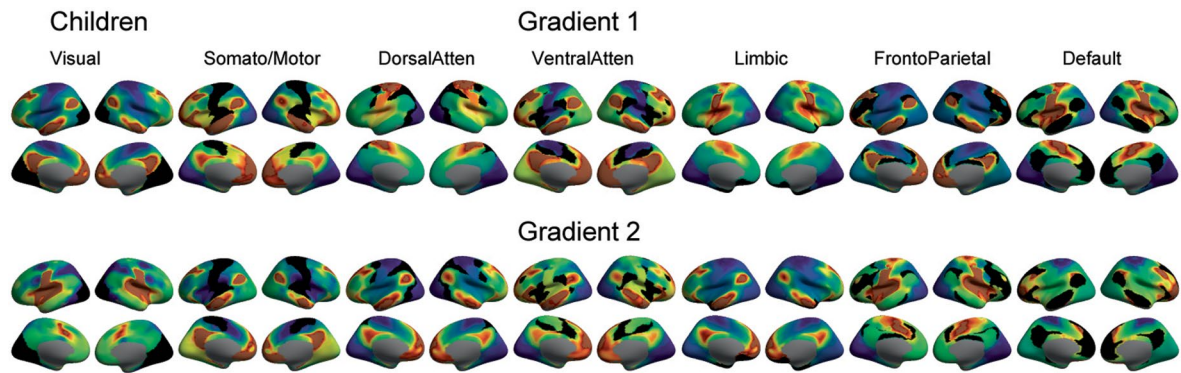
in childhood is highly correlated ( $r=0.9429$ ,  $p<0.01$ , two-sided spin test) with the first gradient that in their adolescence. A consistent group profile that was also evident when considering their second gradients in both childhood and adolescence ( $r=0.9353$ ,  $p<0.01$ , two-sided spin test).





**Extended Data Fig. 3 | Gradient maps in high ventral attention connectivity groups derived from longitudinal data.** A set of child participants ( $n=21$ ) were identified from the high ventral attention group who were also subsequently scanned in their adolescence. Surface maps exhibit a developmentally normative pattern of gradient reversals from their childhood to adolescence. Their first

gradient in childhood was highly correlated with their second gradient in adolescence (absolute  $r=0.9793$ ,  $p<0.01$ , two-sided spin test), while their second gradient in childhood were highly correlated with the first gradient in their adolescence (absolute  $r=0.9748$ ,  $p<0.01$ , two-sided spin test).



**Extended Data Fig. 4 | Gradient maps with functional networks dropped off separately.** Virtual lesion analyses were performed for all the networks respectively. It is revealed that in children group, the drop off of visual, somato/motor, ventral attention and frontoparietal networks generating transmodal organization in the first gradient, while the drop off of dorsal attention, limbic

and default networks conserve the unimodal organization in the first gradient. Readers should interpret these maps with caution as functional networks each contain distinct numbers of vertices along the cortical sheet. Accordingly, the direct examination across the canonical networks, is likely biased by their relative sizes.

## Reporting Summary

Nature Portfolio wishes to improve the reproducibility of the work that we publish. This form provides structure for consistency and transparency in reporting. For further information on Nature Portfolio policies, see our [Editorial Policies](#) and the [Editorial Policy Checklist](#).

### Statistics

For all statistical analyses, confirm that the following items are present in the figure legend, table legend, main text, or Methods section.

- | n/a                                 | Confirmed  |
|-------------------------------------|--|
| <input type="checkbox"/>            | <input checked="" type="checkbox"/> The exact sample size ( $n$ ) for each experimental group/condition, given as a discrete number and unit of measurement  |
| <input type="checkbox"/>            | <input checked="" type="checkbox"/> A statement on whether measurements were taken from distinct samples or whether the same sample was measured repeatedly  |
| <input type="checkbox"/>            | <input checked="" type="checkbox"/> The statistical test(s) used AND whether they are one- or two-sided<br><i>Only common tests should be described solely by name; describe more complex techniques in the Methods section.</i>   |
| <input type="checkbox"/>            | <input checked="" type="checkbox"/> A description of all covariates tested   |
| <input type="checkbox"/>            | <input checked="" type="checkbox"/> A description of any assumptions or corrections, such as tests of normality and adjustment for multiple comparisons  |
| <input type="checkbox"/>            | <input checked="" type="checkbox"/> A full description of the statistical parameters including central tendency (e.g. means) or other basic estimates (e.g. regression coefficient) AND variation (e.g. standard deviation) or associated estimates of uncertainty (e.g. confidence intervals) |
| <input type="checkbox"/>            | <input checked="" type="checkbox"/> For null hypothesis testing, the test statistic (e.g. $F$ , $t$ , $r$ ) with confidence intervals, effect sizes, degrees of freedom and $P$ value noted<br><i>Give <math>P</math> values as exact values whenever suitable.</i>                            |
| <input checked="" type="checkbox"/> | <input type="checkbox"/> For Bayesian analysis, information on the choice of priors and Markov chain Monte Carlo settings  |
| <input checked="" type="checkbox"/> | <input type="checkbox"/> For hierarchical and complex designs, identification of the appropriate level for tests and full reporting of outcomes  |
| <input type="checkbox"/>            | <input checked="" type="checkbox"/> Estimates of effect sizes (e.g. Cohen's $d$ , Pearson's $r$ ), indicating how they were calculated   |

*Our web collection on [statistics for biologists](#) contains articles on many of the points above.*

### Software and code

Policy information about [availability of computer code](#)

- |                 |  |
|-----------------|--|
| Data collection | No software was used during data collection  |
| Data analysis   | Matlab 2018b, Python 2.7, volBrain pipeline ( <a href="https://volbrain.net/">https://volbrain.net/</a> ), Computational Connectome System 1.0 ( <a href="https://github.com/zuoxinian/CCS">https://github.com/zuoxinian/CCS</a> ), ICA-AROMA v3.0 ( <a href="https://github.com/maartenmennes/ICA-AROMA">https://github.com/maartenmennes/ICA-AROMA</a> ), <a href="https://github.com/ThomasYeoLab/ABCD_scripts">https://github.com/ThomasYeoLab/ABCD_scripts</a> ,Freesurfer 6.0, FSL 6.0 and AFNI (17.0.18) were used for data analysis. Code Availability: Code is available online at our GitHub page: <a href="https://github.com/HolmesLab/GradientMaturation">https://github.com/HolmesLab/GradientMaturation</a> . |

For manuscripts utilizing custom algorithms or software that are central to the research but not yet described in published literature, software must be made available to editors and reviewers. We strongly encourage code deposition in a community repository (e.g. GitHub). See the Nature Portfolio [guidelines for submitting code & software](#) for further information.

### Data

Policy information about [availability of data](#)

All manuscripts must include a [data availability statement](#). This statement should provide the following information, where applicable:

- Accession codes, unique identifiers, or web links for publicly available datasets
- A description of any restrictions on data availability
- For clinical datasets or third party data, please ensure that the statement adheres to our [policy](#)

Data from the CCNP dataset used here are available at Chinese Color Nest Project (CCNP) – Lifespan Brain-Mind Development Data Community at Science Data

Bank (<https://ccnp.scidb.cn/en>, <https://doi.org/10.57760/sciencedb.07478> and <https://doi.org/10.57760/sciencedb.07860>). The raw CCNP data are available from the website upon reasonable request.

The ABCD data used in this report came from ABCD BIDS Community Collection (ABCC; NDA Collection 3165) and the Annual Release 2.0: <https://doi.org/10.15154/1503209>.

Source data are provided with this paper.

## Research involving human participants, their data, or biological material

Policy information about studies with [human participants or human data](#). See also policy information about [sex, gender \(identity/presentation\), and sexual orientation](#) and [race, ethnicity and racism](#).

### Reporting on sex and gender

For the CCNP dataset, 176 adolescents (60% female, age range: 6~12 years old) and 202 typically developing children (40% female, age range 12~18 years old). Sex ratio was designed to be balanced in each age group and was collected by self-reporting. All participants and their parents/guardians were informed about the data sharing and provided written informed consent before participating in the study. All phenotypic data has been anonymized and can be publicly accessed at <https://ccnp.scidb.cn/en>.

For the ABCD dataset, 2186 children (female 54.4%, mean age 10.01 years old) were included for the analysis. All participants and their parents/guardians were informed about the data sharing and provided written informed consent before participating in the study. The data can be publicly accessed at <https://abcdstudy.org/scientists/data-sharing/>. Sex were included as covariate variables in the regression analysis.

### Reporting on race, ethnicity, or other socially relevant groupings

No socially constructed or socially relevant categorization variable was used in the current study.

### Population characteristics

Age, sex and head motion during resting-state fMRI were included as covariate variables in the regression analysis.

### Recruitment

For the CCNP dataset, both children and their parents/guardians were approached through lectures that explained this large-scale longitudinal cohorts and popular science activities regarding brain development in local primary and middle schools including students from the first grade of primary school to the second grade of high school.

### Ethics oversight

The reported experiments were approved by the Institutional Review Board from Institute of Psychology, Chinese Academy of Sciences. All participants and their parents/guardians provided written informed consent. The ABCD study was approved by the Institutional Review Board from the University of California, San Diego. All participants and their parents/guardians provided written informed consent.

Note that full information on the approval of the study protocol must also be provided in the manuscript.

## Field-specific reporting

Please select the one below that is the best fit for your research. If you are not sure, read the appropriate sections before making your selection.

Life sciences  Behavioural & social sciences  Ecological, evolutionary & environmental sciences

For a reference copy of the document with all sections, see [nature.com/documents/nr-reporting-summary-flat.pdf](https://nature.com/documents/nr-reporting-summary-flat.pdf)

## Life sciences study design

All studies must disclose on these points even when the disclosure is negative.

### Sample size

MRI brain images (n = 674) were collected from 457 school-age (age range 6–18 years) typically developing children (TDC) of the Chinese Han population. Scans of 176 adolescents and 202 typically developing children were finally included in the current work. CCNP is a five-year accelerated longitudinal study designed to delineate normative trajectories of brain development of Chinese children. Each participant in CCNP is invited to undergo scans three times at nominal 15 month intervals. So far as we knew, CCNP is the largest longitudinal Chinese pediatric MRI dataset. ABCD is a multi-site longitudinal cohort following the brain and cognition development of over ten thousand 9~10 years old children. MRI scans including T1-weighted, T2-weighted and resting-state fMRI was obtained with 3T Siemens Prisma, General Electric 750 and Phillips scanners across 21 sites. Here, we include the MRI baseline data from 2186 children (female 54.4%, mean age 10.01 years old) for the analysis.

As far as we know, up to the time of submission, the CCNP database is the largest longitudinal tracking MRI database of Chinese pediatric population. To address the sample size issue, we then used the ABCD dataset for replication analysis, which includes 2,186 children—almost four times larger than our discovery dataset.

### Data exclusions

Any participant with a history of neurological or mental disorder, family history of such disorders, organic brain diseases, physical contraindication to MRI scanning, a total Child Behavior Checklist (CBCL) T-score higher than 70, or a Wechsler Intelligence Scale for Children IQ standard score lower than 80 were excluded from further analysis. Resting-state data with mean head motion above 0.5mm were excluded in the CCNP dataset. Any resting-state scan with a max head motion above 5 mm and over half of their volumes censored was excluded in the ABCD dataset.

### Replication

The main analysis was performed in the CCNP dataset and replicated with the ABCD dataset in the current study. We found reliable and reproducible results across these two independent datasets.



Randomization	Participants are allocated by age, no randomization was performed.
Blinding	No blinding procedure during data collection, participants are allocated by age, no randomization was performed. For the replication analysis, the data was processed by independent researchers across independent research groups. The CCNP dataset is an open cohort longitudinal study that aims to track the developmental process of children and adolescents. No interventions were applied to the participants, so a double-blind design is not necessary. The group allocation was based on the discovery findings in the current study. The investigators needed to allocate the participants based on a subjective criterion: the degree centrality of the ventral attention network

## Reporting for specific materials, systems and methods

We require information from authors about some types of materials, experimental systems and methods used in many studies. Here, indicate whether each material, system or method listed is relevant to your study. If you are not sure if a list item applies to your research, read the appropriate section before selecting a response.

### Materials & experimental systems

n/a	Involved in the study
<input checked="" type="checkbox"/>	<input type="checkbox"/> Antibodies
<input checked="" type="checkbox"/>	<input type="checkbox"/> Eukaryotic cell lines
<input checked="" type="checkbox"/>	<input type="checkbox"/> Palaeontology and archaeology
<input checked="" type="checkbox"/>	<input type="checkbox"/> Animals and other organisms
<input checked="" type="checkbox"/>	<input type="checkbox"/> Clinical data
<input checked="" type="checkbox"/>	<input type="checkbox"/> Dual use research of concern
<input checked="" type="checkbox"/>	<input type="checkbox"/> Plants

### Methods

n/a	Involved in the study
<input checked="" type="checkbox"/>	<input type="checkbox"/> ChIP-seq
<input checked="" type="checkbox"/>	<input type="checkbox"/> Flow cytometry
<input type="checkbox"/>	<input checked="" type="checkbox"/> MRI-based neuroimaging

## Magnetic resonance imaging

### Experimental design

Design type	resting-state functional MRI
Design specifications	CCNP dataset: resting-state fMRI scan (2x7.45min runs, total 15min 30s), T1 MP-RAGE scan (8min 19s) ABCD dataset: resting-state fMRI scan (4x5min runs, total 20min), T1 MP-RAGE scan (8min 19s)
Behavioral performance measures	No behavioral performance was recorded during scanning.

### Acquisition

Imaging type(s)	resting-state fMRI scan, T1 MP-RAGE scan
Field strength	3 Tesla
Sequence & imaging parameters	CCNP dataset: The T1 weighted scans were acquired with following parameters: flip angle=8°, FOV=256mm, slice number=176, TR/TE=2600/3.02ms, TI=900ms, Voxel size=1.0x1.0x1.0 mm scanning time lasted for 8min 19s. The resting-state scans were acquired with an echo-planar imaging (EPI) sequence using following parameters: flip angle=80°, FOV=216mm, matrix=72x72, slice thickness/gap=3.0/0.33 mm, TR/TE=2500/30ms, slice orientation: sagittal, acquisition direction: interleaved ascending, number of measurements=184, scanning time lasted for 7min 45s.
Area of acquisition	whole brain scan
Diffusion MRI	<input type="checkbox"/> Used <input checked="" type="checkbox"/> Not used

### Preprocessing

Preprocessing software	Matlab 2018b, Python 2.7, Computational Connectome System ( <a href="https://github.com/zuoxinian/CCS">https://github.com/zuoxinian/CCS</a> ), <a href="https://github.com/ThomasYeoLab/ABCD_scripts">https://github.com/ThomasYeoLab/ABCD_scripts</a> , Freesurfer 6.0, FSL 6.0 and AFNI (17.0.18)
Normalization	Volumetric functional data was projected onto fsaverage5 surface template, both linear and non-linear transformations were performed with registration commands implemented in Freesurfer.
Normalization template	fsaverage5 surface template (MNI305 in volumetric space)
Noise and artifact removal	CCNP dataset: (1) dropping the first 10s (4 TRs) for the equilibrium of the magnetic field; (2) estimating head motion parameters and head motion correction; (3) slicing time correction; (4) time series de-spiking; (5) registering functional images to high resolution T1 images using boundary-based registration; (6) removing nuisance factors such as head motion, CSF and white matter signals using ICA-AROMA; (7) removing linear and quadratic trends of the time series; (8) projecting

volumetric time series to surface space (the fsaverage5 model with medial wall masked out); (9) 6mm spatial smoothing. ABCD dataset: (1) dropping the initial frames for the equilibrium of the magnetic field; (2) estimating head motion parameters and voxel-wise differentiated signal variance (DVARs) and head motion correction; (3) registering functional images to high resolution T1 images using boundary-based registration; (4) Scrubbing the frames with  $FD > 0.3$  mm or  $DVARs > 50$ , along with one volume before and two volumes after. (5) removing nuisance factors such as global signal, head motion, CSF and white matter signals; (6) band-pass filtered ( $0.009\text{ Hz} \leq f \leq 0.08\text{ Hz}$ ); (7) projecting volumetric time series to surface space (the fsaverage5 model with medial wall masked out); (8) 6mm spatial smoothing.

Volume censoring

Censoring was applied in the preprocessing of ABCD dataset using MATLAB as following: Scrubbing the frames with  $FD > 0.3$  mm or  $DVARs > 50$ , along with one volume before and two volumes after.

## Statistical modeling & inference

Model type and settings

Whole brain functional connectivity matrix was conducted first, then similarity matrix was generated with only the top 10% FC connections, diffusion map embedding was lastly implemented for dimension reduction.

Effect(s) tested

Whether or not a specific network primarily drives the shift of functional gradient during the transition from childhood to adolescence.

Specify type of analysis:  Whole brain  ROI-based  Both

Statistic type for inference

Voxel-level

(See [Eklund et al. 2016](#))

Correction

Permutation tests were applied to estimate the statistical significance.

## Models & analysis

n/a | Involved in the study

- Functional and/or effective connectivity  
  Graph analysis  
  Multivariate modeling or predictive analysis

Functional and/or effective connectivity

Pearson's Correlation

Graph analysis

Individual-level functional connectivity (FC) matrices and the corresponding Fisher-z transformed values were first generated, which was later averaged across individuals to form group-level FCz matrix. The nodes are vertices in the fsaverage5 space, and edges are FCs between each pair of vertices. Degree centrality map was obtained in binary graph by counting the non-zero elements in each column of the functional connectivity matrix. Later, individual-level degree centrality was used to divide the subjects in to high/low ventral attention connectivity groups.